

## Influence of negative-ion processes on steady-state properties and striations in molecular gas discharges\*

William L. Nighan and W. J. Wiegand

*United Aircraft Research Laboratories, East Hartford, Connecticut 06108*

(Received 11 February 1974)

Theoretical and experimental studies of negative-ion processes in weakly ionized glow discharges have been conducted. Emphasis in these investigations has been directed towards analysis of gas mixtures in which negative ions are produced by dissociative electron attachment of  $\text{CO}_2$ ,  $\text{CO}$ , or  $\text{O}_2$ . It is shown that attachment, detachment, and clustering reactions normally occurring in discharges containing these species can significantly affect both the steady-state and transient characteristics of the plasma, even when an external source of ionization is provided. The magnitude and electron temperature dependence of the electron-molecule attachment coefficient is found to be particularly important. Specifically, analysis shows that when the electron attachment coefficient has a strong positive dependence on electron temperature, and a magnitude exceeding that of the ionization coefficient, an ionization instability can occur. This instability will occur under these circumstances when the negative-ion concentration is comparable to the electron density. Numerical evaluation of the conditions required for this electron-attachment-induced mode of ionization instability results in good agreement with experimentally determined conditions for the onset of striations in gas mixtures for which the charged-particle kinetics can be calculated in detail. In other cases, observed differences between theory and experiment have been related to uncertainties associated with the loss mechanisms of clustered negative ions in the discharge.

### I. INTRODUCTION

Discharges in gas mixtures containing molecular species from which negative ions are readily produced often exhibit behavior which is markedly different from discharges in other gases.<sup>1</sup> The fact that negative-ion processes occurring in such discharges are the cause of the observed behavior has been appreciated for many years.<sup>2,3</sup> However, because of a lack of fundamental data, past attempts to explain the role of negative ions have been largely phenomenological. The present availability of reliable cross-section data for attachment and detachment reactions involving common molecular species now permits rather detailed theoretical analysis of negative-ion processes and their influence on steady-state plasma properties for many experimentally interesting discharges. In this study attention is focused on plasma conditions typical of weakly ionized volume-dominated glow discharges, with emphasis placed on explaining the role of negative-ion processes on discharge behavior. This investigation is limited to gas mixtures in which  $\text{O}^-$  negative ions are initially produced in electron dissociative attachment<sup>4</sup> reactions with  $\text{CO}_2$ ,  $\text{O}_2$ , and  $\text{CO}$ .

An important feature of discharges containing negative ions is the frequent occurrence of unstable behavior which is usually manifested in the form of striations and/or constriction of the plasma. The spatial irregularities resulting from these instabilities can have a highly undesirable effect on plasma behavior, as is often found to be the

case in electric laser applications, for example.<sup>5,6</sup> However, the required understanding of the factors leading to the occurrence of discharge instability is usually lacking. For this reason the present effort has an objective determination and explanation of the initial *causes* of instabilities in charged-particle production and loss processes in molecular discharges when negative ions are present.

In Sec. II basic charged-particle production and loss processes are described. Therein an analysis of attachment and detachment processes is formulated and the influence of these negative-ion processes on steady-state plasma characteristics is discussed. It is shown that attachment and detachment reactions can exert a profound influence on discharge-operating conditions, even when an external source of ionization is employed. In self-sustained discharges the resulting variation of electron temperature can be as much as a factor of 2 for typical gas mixture. Further, it is found that clustering of the initially produced negative-ion species  $\text{O}^-$  with its parent molecule can lead to the formation of stable molecular negative ions. The density of clustered negative ions so produced can become very large, having a significant influence on discharge behavior.

The effect of negative-ion processes on the stability characteristics of glow discharges is analyzed in Sec. III. Therein the results of Sec. II are used to evaluate the criteria for charged-particle production instability as formulated by Haas.<sup>7</sup> The results obtained show that instabilities in the charged-particle production and loss pro-

cesses are likely to occur for experimental conditions which are frequently encountered. Physical interpretation of the factors affecting the criteria for the onset of instabilities indicates that the magnitude and electron temperature dependence of the electron-molecule attachment coefficient is of particular importance as regards the temporal growth of disturbances in the charged-particle densities. Specifically, it has been shown that when the electron and negative-ion densities are comparable, an attachment rate which increases strongly with electron temperature can cause a mode of ionization instability,<sup>8</sup> even when the plasma is sustained by an external source of ionization. Further, the growth rate of this *attachment-induced* ionization instability is strongly peaked in the direction of the steady electric field. This suggests that the ultimate manifestation of this mode of ionization instability will be in the form of a striated plasma.

The experimental factors affecting the occurrence of the previously described instability have been examined in light of the present theoretical findings.<sup>8,9</sup> Several examples of the approach employed to assess the validity of the analytical results are presented in Sec. IV. Therein are discussed the results of experiments utilizing gas mixtures selected such that the important negative-ion reactions were relatively well known. Making use of a convectively cooled discharge with a gas residence time of less than  $10^{-2}$  sec ensured that electron-impact dissociation of the initial species had a minimal effect on mixture composition.<sup>10</sup> For certain easily attainable conditions, the discharges examined were indeed found to be striated,<sup>8</sup> a result interpreted as the manifestation of ionization instability caused by the combined influence of negative-ion production and loss processes. Addition of small concentrations of detaching species to reduce the negative-ion density resulted in the elimination of the striations as predicted. The ability to compute the experimental conditions corresponding to the onset (or elimination) of striations for gas mixtures in which all the important collision processes could be analyzed in detail is taken as evidence that the influence of negative-ion processes on the occurrence of attachment-induced ionization instability is relatively well understood.

In addition to those phenomena which are of central importance to the discussion of Secs. II and III, there are several related aspects of the present subject, detailed analysis of which does not fall within the intended scope of this paper. Of these, the factors determining the validity of a hydrodynamic stability model and the influence of multistep ionization on plasma stability are felt

to be particularly important. These topics are discussed in the Appendix.

## II. ELECTRON AND ION KINETIC PROCESSES

The present investigation has as its primary objective explaining the role of negative ions in glow discharges which are dominated by volume phenomena. Only weakly ionized plasma conditions typical of glow discharges in molecular gases will be explored. The first of these restricting conditions typically limits the application of the following analysis and discussion to discharges having a minimum characteristic dimension on the order of several centimeters, and operating pressures in excess of approximately 10 Torr. That is, the plasma behavior must be dominated by volume processes, with transport phenomena of minor importance. The second constraint requires that the value of fractional ionization not exceed a level of approximately  $10^{-5}$  so that electron collisions with ions and other electrons are not important. For these circumstances, electron energy distributions are generally highly non-Maxwellian,<sup>11,12</sup> with mean electron energies of about 1 eV. In addition, the gas translational temperature is generally well below 1000°K, while the temperature characterizing the vibrational energy density is frequently much higher. Because of the highly nonequilibrium nature of such discharges, the factors influencing electron production, loss, and energy exchange are numerous and complex.<sup>9</sup> In subsequent paragraphs the nature of these processes will be discussed and their influence on steady-state discharge characteristics will be explored in detail. Particular attention will be directed toward assessing the importance of attachment, detachment, recombination, and clustering reactions involving the negative ions, and the subsequent influence of such reactions on electron processes.

### A. Charged-particle production and loss

Charge neutrality is preserved to a high degree in the positive column of glow discharges so that it is necessary to consider only the continuity equations for electrons and negative ions. Further, it will be assumed that single species of negative and positive ions are dominant. Thus, when gradients in plasma properties are unimportant, the electron conservation equation may be expressed in the form

$$\frac{\partial n_e}{\partial t} = n_e n k_i - n_e n_p k_r^e - n_e n k_a + n_n n k_d + n S, \quad (1)$$

where  $n_e$ ,  $n$ ,  $n_n$ , and  $n_p$  are the respective number densities of electrons, neutrals, negative ions,

and positive ions ( $n_p \approx n_e + n_n$ ),  $k_i$  and  $k_a$  are the mixture-weighted electron rate coefficients for *direct* ionization and attachment, averaged over the appropriate electron energy distribution,  $k_r^e$  is the positive-ion-electron recombination coefficient, and  $k_d$  is the mixture-weighted negative-ion detachment coefficient. Thus, for a specific process,

$$k \equiv \sum_j X_j k_j, \quad (2)$$

where  $X_j$  is the fractional concentration of the  $j$ th species in the mixture. In addition, the possible existence of an external independently controllable source of electrons has been included with a rate which is designated  $S$  in Eq. (1). When detachment and recombination are the dominant negative-ion loss processes, the corresponding equation for negative ions is expressed

$$\frac{\partial n_n}{\partial t} = n_e n k_a - n_n n k_d - n_n n_p k_r^i, \quad (3)$$

where  $k_r^i$  is the positive-ion-negative-ion recombination coefficient. Negative-ion clustering reactions are also important for many circumstances of interest. However, many important details of clustering processes are unknown at present. Therefore, reactions involving cluster ion formation and loss are not considered in the present formulation, although their influence is discussed in detail in subsequent sections.

### 1. Electron-molecule ionization and attachment

In weakly ionized discharges, ionization commonly proceeds by way of the single-step process,<sup>9,13,14</sup>  $e + MN \rightarrow MN^+ + 2e$ , while attachment is a dissociative process,<sup>4</sup>  $e + MN \rightarrow M + N^-$ . Electron cross sections for these processes for common diatomic and triatomic species are relatively well known.<sup>4,15-17</sup> In order to determine the rate coefficients for ionization and attachment required for the solution of Eqs. (1) and (3), these cross sections must be properly averaged<sup>11</sup> over the electron energy distribution function  $f$ , i.e.,

$$k_j(E/n) = \left(\frac{2e}{m}\right)^{1/2} \int_0^\infty u f(u, E/n) Q_j(u) du, \quad (4)$$

where  $u$  is the electron energy expressed in electron volts,  $e$  and  $m$  are the electronic charge and mass,  $Q_j(u)$  is the cross section for the process in question, and  $E/n$  is the ratio of electric field intensity to total neutral-particle number density. Since the electron energy distribution depends on  $E/n$  and gas mixture, electron rate coefficients are also dependent on these properties. For a specific mixture  $E/n$  is uniquely related to the

mean electron energy characteristic of the electron energy distribution function. Thus it is convenient to introduce the generalized electron temperature (or reduced average energy<sup>11</sup>) defined by the relation

$$T_e(E/n) \equiv \frac{2}{3} \bar{u} = \frac{2}{3} \int_0^\infty u^{3/2} f(u, E/n) du, \quad (5)$$

where  $T_e$  is expressed in electron volts. Throughout the discussion to follow, the electron rate coefficients  $k_j$  will be related to electron temperature by way of Eqs. (4) and (5).

Numerical computations<sup>11</sup> of ionization and attachment coefficients for several common molecular species have shown that the electron temperature dependence of these rate coefficients is not unduly sensitive to variations in the electron energy distribution resulting from changes in gas mixture. Therefore, throughout the present paper the primary species of interest,  $\text{CO}_2$ ,  $\text{O}_2$ , and  $\text{CO}$ , will be considered in mixtures containing relatively large quantities of  $\text{N}_2$  and  $\text{He}$ . For reasons to be elaborated upon in Sec. IV, it has been found that maintaining a substantial background of  $\text{N}_2$  and  $\text{He}$  in the mixture provides an element of control which is particularly useful when interpreting experimental and theoretical data. Further, mixtures of this general type are of special interest because of their application in electric discharge lasers.<sup>5</sup> It should be emphasized, however, that the results and interpretation of subsequent sections are of a general nature, and therefore their application is not limited to specific gas mixtures.

Presented in Figs. 1 and 2 are computed ionization and attachment rate coefficients for a number of common molecular species. The ionization coefficients for the species indicated all have a very strong dependence on electron temperature, a rather general result. However, while certain of the attachment rate coefficients have a similarly strong dependence on electron temperature, others do not. For those species such as  $\text{CO}_2$ ,  $\text{O}_2$ ,  $\text{CO}$ ,  $\text{NO}$ , and  $\text{H}_2\text{O}$  for which the dissociative attachment process has an energy threshold<sup>4</sup> at least a few electron volts higher than typical values of discharge electron temperature, the coefficients for ionization and attachment have comparable magnitudes and electron temperature dependences. However, for certain oxides of nitrogen and other species as well, the energy threshold for dissociative attachment occurs at a very low electron energy. This, coupled with large values of the attachment cross-section,<sup>4</sup> results in attachment coefficients which are sensibly independent of electron temperature and much larger than their corresponding ionization coefficients.

The relative magnitudes and electron tempera-

ture dependences of the ionization and attachment coefficients shown in Figs. 1 and 2 have a fundamental influence on discharge stability. Therefore it is convenient to define a parameter reflecting the electron temperature dependence of a rate coefficient independent of its magnitude. The fractional, or logarithmic, derivative with respect to electron temperature is useful for this purpose, i.e.,

$$\hat{k} \equiv \frac{T_e}{k} \frac{\partial k}{\partial T_e} = \frac{\partial \ln k}{\partial \ln T_e}; \quad (6)$$

for example, if  $k \propto T_e^{10}$  then  $\hat{k} = 10$ . Thus, throughout the remainder of this paper the *caret* notation will be used as a shorthand representation of the indicated logarithmic derivative taken with respect to electron temperature. For the species corresponding to the data of Figs. 1 and 2 all the

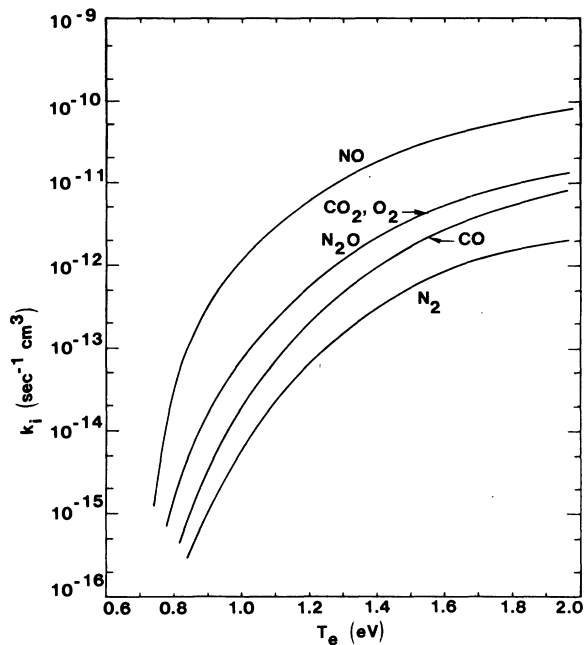


FIG. 1. Electron-molecule ionization coefficients computed using electron energy distributions for a  $\text{CO}_2$ - $\text{N}_2$ -He mixture in the number density proportions 0.05:0.35:0.60. The rate coefficients for all species other than  $\text{CO}_2$  and  $\text{N}_2$  are strictly applicable only for these species as minority constituents in a  $\text{CO}_2$ - $\text{N}_2$ -He mixture having the proportions indicated. While the values of the rate coefficients for each species at a specific electron temperature will change as mixture composition is varied, calculations have shown that the relative relationship between the various coefficients is only slightly affected. For the conditions of this figure the ionization coefficients for  $\text{CO}_2$ ,  $\text{O}_2$ , and  $\text{N}_2\text{O}$  are within approximately 10–20% of one another over the entire electron temperature range shown. Thus a single curve representing these three species is presented as indicated.

values of  $\hat{k}_i$  are in the range 10–30, depending on  $T_e$ , while the values of  $\hat{k}_a$  range from approximately zero to 20, reflecting the relationship between the attachment energy threshold and electron temperature as discussed above.

## 2. Recombination processes

The species of positive and negative ion produced by the reactions corresponding to the data of Figs. 1 and 2 are well known.<sup>4,15</sup> However, these ions engage in a host of very fast charge-exchange and rearrangement reactions involving both the primary neutral species and neutral minority species produced in the discharge as a result of dissociation and other plasma chemical processes.<sup>9</sup> Thus knowledge of the dominant species of positive and negative ion in discharges is frequently uncertain. In addition, the exact magnitude and energy dependence of the rate coefficients<sup>18–22</sup> for electron-ion recombination processes, which proceed by way of the dissociative reaction  $e + MN^+ \rightarrow M + N$ , are not well known for many likely species of ions. Table I summarizes several typical electron-positive-ion recombination processes, their magnitudes, and their dependence on electron temperature. In spite of the

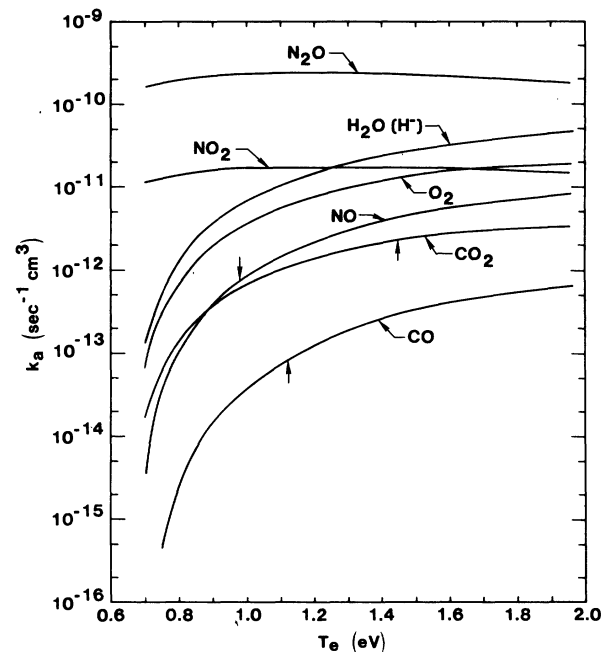


FIG. 2. Electron-molecule rate coefficients for dissociative attachment computed using electron energy distributions for the mixture of Fig. 1. Except as indicated for  $\text{H}_2\text{O}$  (see Ref. 16) the negative ion resulting from these processes is  $\text{O}^-$ . The vertical arrows denote the point at which  $k_i$  is equal to  $k_a$ . For  $\text{O}_2$ ,  $k_i$  equals  $k_a$  in this mixture for  $T_e \sim 2.1$  eV.

uncertainties associated with the details of electron-ion recombination processes, the variation in magnitude of the rate coefficients given in the table is more than compensated for by the fact that values of  $\hat{k}_r^e$  are very much less than those for  $\hat{k}_i$  and  $\hat{k}_a$ . Thus it is found that both steady-state and transient plasma characteristics are not very sensitive to the precise nature of the positive ion species.

Positive-ion-negative-ion recombination processes<sup>22-26</sup> suffer from the same lack of complete understanding indicated above in connection with electron-ion recombination. Probable reactions of importance for the discharge conditions of present interest are also summarized in Table I. While the relative concentrations of weakly bound cluster ions<sup>27,28</sup> are likely to be very sensitive to gas temperature variations and possibly to reactions involving excited molecular species, such effects are not considered in the present analysis.

### 3. Detachment and clustering processes

It is interesting to note that, with the exception of H<sub>2</sub>O,<sup>16</sup> the dissociative attachment reactions corresponding to the data of Fig. 2 all lead to the production of the same negative ion, O<sup>-</sup>. Rate

coefficients for the detachment of the electron from O<sup>-</sup> by way of the associative detachment reaction  $MN + O^- \rightarrow MNO + e$  are well known for a number of effective detaching species<sup>28-32</sup> (Table I). However, it is notable that for many experimentally interesting situations the principal species<sup>28,30</sup> in the mixture cannot detach electrons from O<sup>-</sup>. In addition, clustering of O<sup>-</sup> with the molecule from which it was initially produced<sup>28,33,34</sup> frequently occurs on a time scale which is much faster than that typical of likely detachment reactions. Thus, as indicated by the data of Fig. 3, three-body clustering reactions can very rapidly convert the initial species of negative ions to more stable cluster ions.<sup>9</sup> The high electron affinity and/or the greater cluster bond energy of many stable cluster ions makes the removal of the electron by collisional detachment<sup>35-37</sup> or by dissociation back to O<sup>-</sup>, from which the electron is subsequently detached, relatively more difficult. Of specific importance to this study is the fact that some of the more common O<sup>-</sup> detaching species such as CO are ineffective in destroying CO<sub>3</sub><sup>-</sup> cluster negative ions.<sup>34</sup> The effects of clustering reactions on plasma characteristics will be discussed in subsequent sections.

TABLE I. Ion loss processes.

Reaction type	Rate coefficient <sup>a</sup> (cm <sup>3</sup> -sec <sup>-1</sup> )	Reference <sup>a</sup>
<b>Dissociative recombination</b>		
$e + CO_2^+ \rightarrow CO + O$	$\sim 6 \times 10^{-8}$ , <sup>b</sup> $T_e \approx 1$ eV	(20), 21, 22
$e + O_2^+ \rightarrow O + O$	$\sim 2 \times 10^{-8}$ , <sup>b</sup> $T_e \approx 1$ eV	(18), 21, 22
$e + NO^+ \rightarrow N + O$	$\sim 7 \times 10^{-8}$ , <sup>b</sup> $T_e \approx 1$ eV	(19), 21, 22
<b>Positive-negative ion recombination</b>		
$O^- + O_2^+ \rightarrow O + O_2$	$1 \times 10^{-7}$	22, 23, (26)
$O^- + NO^+ \rightarrow O + NO$	$4.9 \times 10^{-7}$	22, 23, (26)
$NO_2^- + NO^+ \rightarrow NO_2 + NO$	$5.1 \times 10^{-7}$	24, (25)
<b>Associative detachment</b>		
$O^- + CO \rightarrow CO_2 + e$	$7.3 \times 10^{-10}$	28, 29, 30, 32, (34)
$O^- + O \rightarrow O_2 + e$	$2 \times 10^{-10}$	30, (31)
$O^- + O_2 \rightarrow O_3 + e$	$< 10^{-12}$	30
$O^- + O_2(a^1\Delta_g) \rightarrow O_3 + e$	$\sim 3 \times 10^{-10}$	(31), 32
$O^- + NO \rightarrow NO_2 + e$	$5 \times 10^{-10}$	28, 29, (30)
$O^- + H_2 \rightarrow H_2O + e$	$7.5 \times 10^{-10}$	28, (29), 30, 32
$O^- + CO_2 \rightarrow CO_2 + O + e$	$< 4 \times 10^{-12}$	28
$O^- + N_2 \rightarrow N_2O + e$	$< 10^{-12}$	30
$O^- + He \rightarrow He + O + e$	Small, endothermic	
$CO_3^- + CO \rightarrow 2CO_2 + e$	$< 10^{-13}$	34
<b>Negative ion clustering<sup>c</sup></b>		
$O^- + CO_2 + M \rightarrow CO_3^- + M$	$1.1 \times 10^{-27}$ , $M = CO_2$	28, (34), 41
$O^- + O_2 + M \rightarrow O_3^- + M$	$1.05 \times 10^{-30}$ , $M = O_2$	28, (33)

<sup>a</sup>The quoted rate coefficient was obtained from the reference in parentheses.

<sup>b</sup>The recombination coefficients at  $T_e \approx 1$  eV were obtained by extrapolation of existing measurements (O<sub>2</sub><sup>+</sup>) or by estimates from the  $T = 300$  °K rate based on the  $T_e^{-1/2}$  dependence (Ref. 21).

<sup>c</sup>The units for these three-body rate coefficients are cm<sup>6</sup>sec<sup>-1</sup>.

### B. Steady-state operating conditions

The value of  $E/n$ , and therefore electron temperature, required to sustain a collision-dominated molecular discharge at a particular current density is determined by the relationship between the electron production and loss processes.<sup>9</sup> For the conditions of interest the attachment-detachment processes can vary greatly leading to as much as a factor-of-2 variation in the sustaining value of  $E/n$ . Since many plasma properties are exceedingly sensitive to the corresponding changes in electron temperature, the resultant effects of negative-ion kinetic processes can be of considerable significance.

One of the primary reasons for the strong influence on plasma behavior of attachment and detachment processes is illustrated by the data shown in Fig. 4. Presented in the figure are the  $\text{CO}_2$  ionization and attachment coefficients computed for a representative gas mixture in which both processes are dominated by electron- $\text{CO}_2$  collisions. Also shown is the electron-ion recombination coefficient weighted by the fractional ionization  $n_p/n$ , as suggested by the form of Eq.

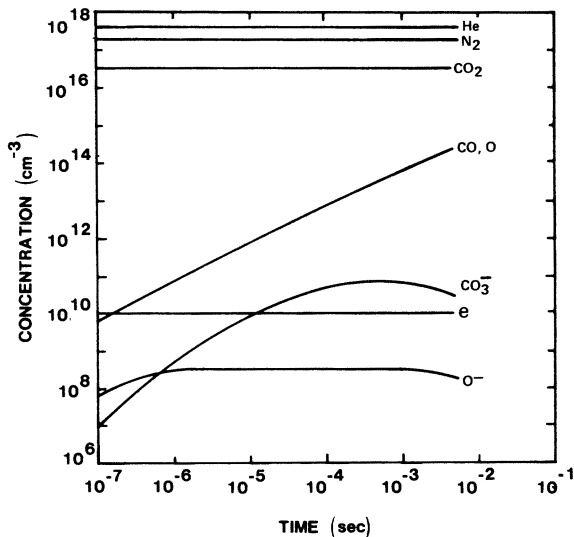


FIG. 3. Temporal evolution of  $\text{CO}_2$  dissociation fragments and the negative ions  $\text{O}^-$  and  $\text{CO}_3^-$  as computed in Ref. 9. The mixture is that of Fig. 1 at a pressure of 20 Torr and a constant electron density of  $10^{10} \text{ cm}^{-3}$ . The computation simulates conditions after entrance of the initial mixture into the region of a steady self-sustained convection discharge. In the calculation of the  $\text{CO}_3^-$  density, only loss reactions involving unexcited species were considered, whereas the experimental data discussed in Sec. IV indicate that collisions with excited species may significantly affect the relative  $\text{CO}_3^-$  and  $\text{O}^-$  concentrations under actual discharge conditions (see Ref. 55 also).

(1). Various possible steady-state operating conditions will now be examined.

#### 1. Self-sustained discharge—no detachment

When detachment is unimportant, positive-ion-negative-ion recombination balances attachment. Thus the steady-state form of Eq. (1) indicates that in this limit

$$k_i = k_a + (n_p/n) k_r^e. \quad (7)$$

Examination of Fig. 4 shows that in this “no-detachment” limit  $k_a \gg (n_p/n) k_r^e$ , for almost any reasonable value of fractional ionization and/or recombination coefficient. Therefore, self-sustained discharge operation requires that ionization balance the entire loss of electrons due to attachment, i.e.,  $k_i \approx k_a$ . This occurs for an electron temperature of approximately 1.5 eV (point a) for the conditions of Fig. 4, a value not unduly sensitive to mixture changes. In fact, analysis shows that over a broad range of conditions in which either  $\text{CO}_2$ ,  $\text{O}_2$ , or  $\text{CO}$  is present in signifi-

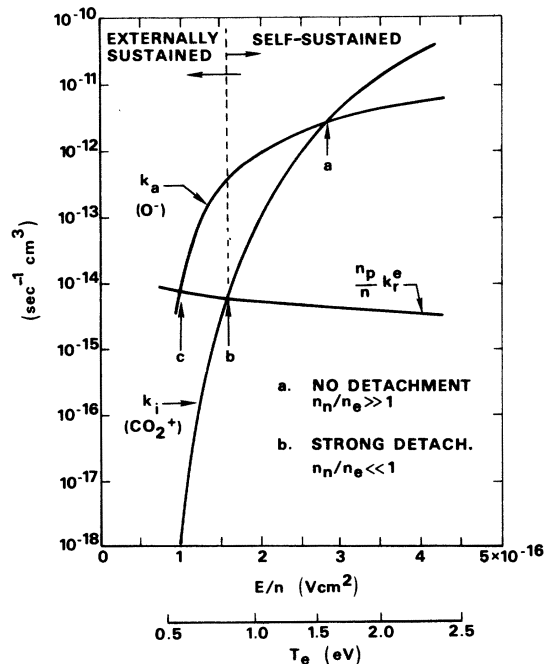


FIG. 4. Illustrative comparison of electron coefficients for ionization, attachment, and recombination for representative discharge conditions for which ionization and attachment processes are dominated by  $\text{CO}_2$ . The weighted recombination coefficient is typical of a fractional ionization value of approximately  $10^{-7}$ . Compared to the important effects of detachment as discussed in the text, the indicated discharge-operating regions are not particularly sensitive to variations in the electron energy distribution, fractional ionization, or positive-ion species.

cant quantity, the condition  $k_i \approx k_a$  for mixture-weighted coefficients occurs in the 1.0–2.0-eV range of electron temperatures. Discharge operation for conditions typical of point *a* in Fig. 4 is likely to be realized when (i) the density of species capable of detaching  $O^-$  is very low, or (ii)  $O^-$  instantaneously clusters to form a very stable ionic species such as  $CO_3^-$  or  $O_3^-$ . Denes and Lowke<sup>38</sup> have recently measured operating characteristics of pulsed  $CO_2$  laser discharges and have found that operating values of  $E/n$  do correspond to the condition  $k_i = k_a$ , point *a* in Fig. 4. As indicated in the figure, the concentration of negative ions relative to the electrons will be large for conditions representative of point *a*.

### 2. Self-sustained discharge—strong detachment

If the density of a detaching species such as CO is large enough to immediately convert  $O^-$  back to  $CO_2$  and a free electron, attachment-detachment kinetics will have a negligible effect on steady discharge properties. In this limit the steady negative-ion density will be small and positive-ion–negative-ion recombination will be unimportant compared to detachment. Thus Eq. (3) indicates that attachment is balanced by detachment,

$$k_a = (n_n/n_e) k_d, \quad (8)$$

while Eq. (1) shows that ionization balances recombination,

$$k_i = (n_p/n) k_r^e, \quad (9)$$

as would be the case in the absence of negative-ion processes. When this situation occurs, the discharge can be sustained at a much lower value of electron temperature, viz., point *b* in Fig. 4.

Of course the entire region between points *a* and *b* is experimentally accessible. Since CO is a very effective detaching species and is readily produced by electron-impact dissociation<sup>39</sup> in discharges containing  $CO_2$  (Fig. 3), the discharge-operating point is greatly influenced by the value of the CO fractional concentration,  $f \equiv [CO] / ([CO_2] + [CO])$ . In sealed or slow-flow discharges<sup>10</sup> containing  $CO_2$  in which CO has time to accumulate to the point where  $f \gtrsim 0.1$ , the influence of detachment is very strong so that negative-ion processes are likely to be insignificant. However, in fast-flow<sup>10</sup> convection-dominated discharges of the type commonly utilized in electric laser applications, the gas residence time in the discharge is frequently  $10^{-2}$  sec or less, a time insufficient for the CO fraction to exceed approximately 0.10. Further, the extent of the  $CO_2$  dissociation depends on electron density which is, of course, a variable quantity in discharges. Thus for typical  $CO_2$  convection-discharge conditions,  $f$  varies in the

approximate range  $10^{-4}$ – $10^{-1}$  depending on circumstances, thus shifting the discharge-operating point in the region between points *a* and *b* in Fig. 4.

### 3. External ionization

Interest in the development of high-pressure glow discharges for laser applications has led to the development of high-energy electron beam and photoionization sources for the purpose of providing uniform ionization in large volumes.<sup>40</sup> When an independently controllable source of ionization is provided, the electron temperature can be maintained at a value independent of electron production and loss processes by adjusting the value of the applied electric field, i.e.,  $E/n$ . Usually conditions are selected so that the ionization resulting from direct low-energy electron impact is insignificant compared to that provided by the auxiliary source, i.e.,  $S \gg n_e k_i$  (Eq. 1). Therefore, for a specific mixture the value of  $E/n$  is selected such that the discharge operates to the left of point *a* in Fig. 4, and usually to the left of point *b*. However, Fig. 4 indicates that there exists a rather broad range of electron temperature values extending below the minimum value required for self-sustained operation (point *b*) within which attachment may be the dominant electron loss process, depending on the importance of detachment. When detachment is insignificant, as may occur for the reasons cited previously, the electron temperature must be maintained at a value below that corresponding to point *c* if the plasma is to be recombination dominated, i.e.,  $(n_p/n)k_r^e \gg k_a$ . The primary reason for providing the ionization with an external source is to ensure a high degree of spatial uniformity and stability, which implies that *both* electron production and loss processes are relatively insensitive to variations in electron temperature and therefore  $E/n$ . Clearly, in the electron temperature region between points *b* and *c* in Fig. 4, which is accessible only when auxiliary ionization is provided, the electron loss process may remain a very strong function of electron temperature. Such a strong dependence on electron temperature may lead to instability, as will be discussed in Sec. III.

#### C. Steady-state electron temperature variations

Frequently, the principal species which can cause negative-ion detachment are not present in the initial discharge mixture. For example, the CO content in mixtures containing  $CO_2$  results as a consequence of direct electron-impact dissociation of  $CO_2$  (Fig. 3), and therefore depends on current density, electron temperature, and, in convection discharges, on residence time in the

discharge region.<sup>9,39</sup> In order to illustrate the influence of detachment on the steady-state value of electron temperature, the time-independent forms of Eqs. (1) and (3) were solved numerically for several gas mixtures. Figure 5 presents the computed electron temperature values for two gas mixtures in which CO is presumed to have been added as a detaching agent. The rate coefficients used for recombination and detachment processes are those given in Table I, while the mixture-weighted electron-molecule rate coefficients for ionization and attachment were obtained using computed electron energy distributions appropriate for each mixture. Because of the large fractional concentration of  $N_2$  in both mixtures, electron energy exchange processes and therefore the electron energy distributions were entirely dominated by the  $N_2$ . However, ionization and attachment reactions were dominated by  $CO_2$  and  $O_2$  in the respective mixtures. In the computation of the data of Fig. 5 negative-ion clustering reactions were *not* included. Thus, for the purpose of this illustration  $O^-$  is always considered to be the dominant negative-ion species.

For very low values of CO content ( $f \lesssim 10^{-4}$ ) detachment is unimportant in both mixtures so that ionization must balance the entire electron loss due to attachment. Since  $O_2$  has a substantially higher attachment rate than  $CO_2$  (Fig. 2), a larger value of electron temperature is required to sustain the  $O_2$  mixture in the absence of detachment. Rapid CO production due to dissociation normally occurring in  $CO_2$  mixtures does not usually permit steady

operation in this no-detachment limit (see Fig. 3). However, measurements<sup>38</sup> of  $E/n$  in pulsed  $CO_2$  discharges in which CO accumulation is very small correspond to electron temperature values for which ionization balances attachment,  $k_i = k_a$ . Thus, the methods used to establish the electron temperature values corresponding to the left-hand portion of Fig. 5 are supported by experimental observations. As the CO content is increased, detachment increases in importance, partially offsetting the effect of attachment, with the result that  $T_e$  decreases. Ultimately, sufficient CO is present to entirely offset the effect of attachment and the plasma becomes recombination dominated for both mixtures. In this limit electron temperature values have been inferred from measurements of  $E/n$  using the techniques described in Sec. IV. For both mixtures the electron temperature values so obtained were found to be within  $\sim 5\%$  of the computed values as indicated by the data points in Fig. 5.

The sequence of events causing the decrease in electron temperature with increasing CO content for the  $CO_2$  mixture corresponds to the transition from point *a* to point *b* in Fig. 4. However, it will be shown in Sec. III that a smooth steady transition from attachment to recombination domination as suggested by the data of Fig. 5 is not always possible, due to the occurrence of plasma instability.

#### Negative-ion clustering reactions

In the calculations leading to the results presented in Fig. 5, the three-body clustering reactions  $O^- + O_2 + M \rightarrow O_3^- + M$  and  $O^- + CO_2 + M \rightarrow CO_3^- + M$  were not taken into account because the subsequent chain of reactions affecting such cluster ions is not known at present. However, the rate coefficients for the initial step in the formation of the indicated cluster reactions are known (Table I). Comparison of these coefficients with the  $CO-O^-$  detachment coefficient indicates that the clustering and detachment reactions will be of comparable importance for the  $O_2$  mixture of Fig. 5 when  $f \sim 10^{-3}$ , and for the  $CO_2$  mixture<sup>41</sup> for  $f \sim 10^{-1}$ . Thus the calculated results for the transition from attachment to recombination domination for the  $O_2$  mixture are expected to be reasonably quantitative as regards the CO fractional concentration scale. However, because of the very fast  $O^-$  clustering reaction involving  $CO_2$ , the fractional CO concentration will have to reach a level above  $10^{-1}$  before the CO detachment reaction can effectively compete with the  $CO_3^-$  cluster formation. Therefore, the qualitative trend exhibited by the data of Fig. 5 for the  $CO_2$  mixture is likely to occur for values of CO fraction nearly 100 times larger than the

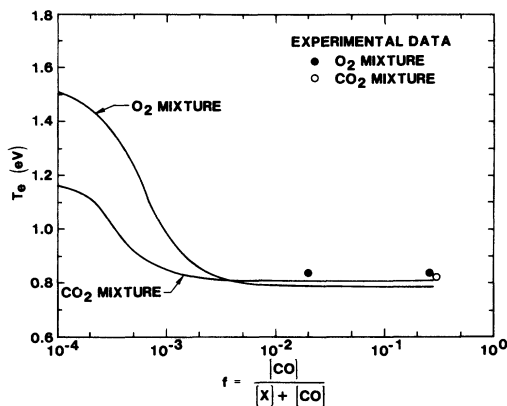


FIG. 5. Computed steady-state electron temperature values for  $X-N_2-He$  mixtures having the number density proportions 0.05:0.35:0.60, where  $X$  represents either  $CO_2$  or  $O_2$ . The calculations were made for a total pressure of 20 Torr and an electron density of  $10^9 \text{ cm}^{-3}$ . Electron temperatures inferred from  $E/n$  measurements in steady discharges at these conditions are shown. As indicated in the text, negative-ion clustering reactions were not taken into account in the calculations.



values shown. In addition to the obvious effect on the steady-state properties of the plasma, the influence of this clustering process can be significant as regards plasma stability characteristics, a subject which will be discussed below.

### III. CHARGED-PARTICLE MODES OF INSTABILITY

The development presented in Sec. II indicates that the *net* effect of negative-ion production and loss can significantly alter steady-state plasma conditions by introducing a variable loss process for electrons that must be balanced whether the plasma is self-sustaining or is sustained by an external source of ionization. However, the influence of negative-ion processes on the response of plasma properties to a disturbance can be even more significant, especially when detachment permits discharge operation at electron temperature values for which the magnitude of the attachment coefficient exceeds that of the ionization coefficient, i.e., to the left of point *a* in Fig. 4. In the discussion to follow, the influence of negative-ion processes on the plasma response to a small amplitude disturbance will be analyzed. On the basis of the results discussed in Sec. II, criteria for the stability of charged-particle production and loss processes as formulated by Haas<sup>7</sup> will be applied for a range of discharge conditions. In particular, it will be shown that a detailed understanding of the unperturbed plasma state (Sec. II) is essential to any meaningful evaluation of the theoretical stability criteria.

#### A. Theoretical considerations

It is known that the wavelike disturbances (striations) frequently observed in discharges are a manifestation of a plasma instability related to the ionization process.<sup>42,43</sup> Further, the influence of negative-ion processes on the ionization mechanism has been postulated<sup>42-44</sup> as having an important part in the development of this instability in molecular gas discharges. However, attempts to explain the effects of negative-ion process on plasma stability have, for the most part, been limited to phenomenological discussions. Recently Haas<sup>7</sup> analyzed the general stability characteristics of volume-dominated discharges in molecular gases containing negative ions using a self-consistent model of discharge processes. On the basis of that study it was determined that several different wave modes can be excited under typical conditions, including those resulting from amplification of disturbances in the charged-particle production and loss processes. For the purposes of the present study the theoretically derived<sup>7</sup> criteria for instability of charged-particle modes

in discharges containing negative ions are of primary importance. Those features of Haas's analysis and interpretation which are pertinent to this investigation are summarized in the discussion to follow.

#### 1. Time scales

As pointed out in Ref. 7, analysis of the temporal evolution of the normal wave modes characterizing the response of a plasma to a disturbance requires careful consideration of the time ranges within which basic properties can change. For the discharge conditions of interest the characteristic times representative of changes in the electron and ion concentrations,  $(nk_i)^{-1}$ ,  $(n_p k_r)^{-1}$ ,  $(nk_a)^{-1}$ ,  $(nk_d)^{-1}$ , . . . , are typically in the range  $10^{-8}$ – $10^{-4}$  sec. Neutral-particle properties do not respond on this time scale and are therefore effectively frozen during the time required for the *initial development* of a disturbance in the charged-particle production processes. By way of contrast, space-charge relaxation occurs on a much shorter time scale ( $10^{-10}$ – $10^{-9}$  sec) so that the space-charge fluctuation is small compared to the electron and ion density fluctuations.<sup>7</sup> Thus the relevant system of equations to be analyzed in connection with an investigation of charged-particle production instability includes the continuity equations for electrons and negative ions [Eqs. (1) and (3)], Maxwell's equations, and the electron energy equation. Since evaluation of basic *unperturbed* plasma properties characterizing the initial or onset phase of disturbance development is the primary objective here, these equations are linearized in the usual fashion by introducing small deviations of the plasma variables from their steady-state values in the manner described in Refs. 7 and 42. The more important aspects of this approach are discussed in the following paragraphs.

#### 2. Perturbed plasma properties

In collision-dominated plasmas the time-dependent electron energy conservation equation to be used along with Eqs. (1) and (3) may be expressed in the form

$$\frac{\partial}{\partial t} \left( \frac{3}{2} n_e k T_e \right) = \vec{J}_e \cdot \vec{E} - n_e n \left( \frac{\nu_u}{n} \right) k T_e, \quad (10)$$

where  $\vec{J}_e$  is the electron current density vector and  $\nu_u$  is the total electron energy exchange-collision frequency, which depends on electron temperature. Since the electron current density can be expressed in terms of electron density, electron temperature, and electric field intensity,<sup>7</sup> the plasma properties considered to undergo small amplitude perturbations are the electron density and temperature, the

negative-ion density, and the electric field intensity. The perturbations in these quantities are represented by a linear superposition of plane waves of the form<sup>7,42,45,46</sup>

$$\psi_k e^{i(\omega t - \vec{k} \cdot \vec{x})}, \quad (11)$$

where  $\omega$  is the complex wave frequency  $\omega = \omega_r + i\omega_i$ ,  $\vec{k}$  is the wave vector ( $2\pi/\text{wavelength}$ ),  $x$  is the spatial variable, and  $\psi_k$  is the amplitude of the  $k$ th Fourier component of a specific property, e.g.,  $T_{e_k}$ ,  $n_{e_k}$ ,  $n_{n_k}$ , and  $\vec{E}_k$ . Analysis of the stability of the plasma requires development of an equation for  $\omega$  in terms of the unperturbed steady-state properties of the plasma using the first-order expansions of Eqs. (1), (3), and (10). The complex roots of the resulting equation can each be identified with a potential mode of unstable plasma behavior. For a specific root  $\omega_\alpha$  the relationship coupling  $\text{Re}(i\omega_\alpha)$ ,  $\vec{k}$ , and the unperturbed plasma properties determines the temporal evolution of a disturbance; i.e., if  $\text{Re}(i\omega_\alpha) > 0$  disturbances grow in time, indicative of instability.<sup>46</sup> Thus  $\text{Re}(i\omega_\alpha)$  is the growth (or damping) rate of a disturbance. Similarly, the equation relating  $\text{Im}(i\omega_\alpha)$ ,  $\vec{k}$ , and the steady plasma properties reveals the nature of the propagation or dispersion characteristics of the waves.<sup>45</sup> Clearly, the sign of the equation involving  $\text{Re}(i\omega_\alpha)$  for a specified root is of primary importance, for it determines the occurrence of unstable plasma behavior. However, as will become apparent, the equation reflecting the temporal evolution of a disturbance frequently contains numerous complicated terms of varying sign, the magnitudes of which are usually much greater than their sum. For this reason, generation and evaluation of valid expressions for the disturbance growth rate  $\text{Re}(i\omega_\alpha)$  are generally much more difficult and sensitive to the methods used and processes considered than is the case for the corresponding equations for  $\text{Im}(i\omega_\alpha)$ . The present investigation is directed toward determination of the basic causes of disturbance growth rather than investigation of the dispersion characteristics of the unstable waves. Thus in the sections to follow only those equations for the temporal component,  $\text{Re}(i\omega_\alpha)$ , will be analyzed.

### 3. Quasisteady electron energy kinetics

Because there are three time derivatives involved in the first-order expansions of Eqs. (1), (3), and (10), the relevant equation for  $\omega$  is generally a complicated third-order polynomial. Consideration of more than one species of positive or negative ion would further increase the order of the equation. However, recognition of the sig-

nificance of the relationships among the time scales discussed above permits meaningful reduction of the order of the equation. In mixtures of molecular gases of the type under consideration, the characteristic time for electron energy relaxation,  $\nu_u^{-1}$ , is very short ( $10^{-10}$ – $10^{-8}$  sec) relative to the time required for ionization, attachment, etc., owing to the large low-energy electron rates for vibrational excitation.<sup>11</sup> Thus the temporal response of the electron energy density to a local disturbance is effectively instantaneous as compared to the time required for changes in the charged-particle densities. The relationship between these characteristic response times permits omission of the time derivative in the perturbed form of Eq. (10) when analyzing the temporal development of disturbances in the charged-particle production and loss process, thereby reducing the order of the equation for  $\omega$  by 1. This does not imply that the electron energy density remains unchanged in the  $10^{-8}$ – $10^{-5}$ -sec time range required for the charged-particle densities to respond to a disturbance. Rather, the electric field, electron temperature, electron density, and electron-temperature-dependent collision frequencies, and therefore the electron energy density, rapidly readjust to a disturbance on the time scale of interest. Therefore the first-order perturbed form of the electron energy equation can be considered to be time independent and can be used to provide a quasisteady relationship between the perturbation amplitudes  $T_{e_k}$ ,  $n_{e_k}$ , and  $\vec{E}_k$ .

As mentioned previously, relaxation of disturbances in the charge density occurs on a time scale even shorter than that typical of electron energy relaxation. Examination of Maxwell's equations reveals that the quasineutral<sup>7</sup> nature of the plasma response to a disturbance developing on the time scale typical of the ionization process indicates that  $\nabla \cdot \vec{J}_{e_k} \approx 0$  when the ions are considered infinitely massive. Application of this relationship, and consideration of the fact that disturbances in the electric field are irrotational when electromagnetic phenomena are unimportant, as in the present case, provides the information required to eliminate the amplitude  $\vec{E}_k$  from the quasisteady electron energy equation.<sup>7</sup> There results a single relationship expressing the coupling between the amplitude of perturbations in electron temperature and density.

For conditions such that volume processes dominate plasma behavior, Haas has developed the mathematical formulation descriptive of the previous discussion and has shown (Sec. IV C of Ref. 7) that the quasisteady relationship coupling the perturbation amplitudes  $T_{e_k}$  and  $n_{e_k}$  is expressed by the relation

$$\frac{T_{e_k}}{T_e} = \left( \frac{-2 \cos^2 \phi}{1 + \hat{\nu}_u - \hat{\nu}_m \cos 2\phi} \right) \frac{n_{e_k}}{n_e} \equiv \left( \frac{-2 \cos^2 \phi}{\hat{\nu}'_u} \right) \frac{n_{e_k}}{n_e}, \quad (12)$$

where  $\nu_m$  is the electron momentum-transfer collision frequency,  $\phi$  is the angle between the direction of the steady-state electron current density and the direction of the wave-propagation vector as illustrated in Fig. 6, and  $\hat{\nu}'_u$  is defined as  $1 + \hat{\nu}_u - \hat{\nu}_m \cos 2\phi$ . The *caret* notation refers to the logarithmic derivative taken with respect to electron temperature as described in connection with Eq. (6). Clearly the sign of  $\hat{\nu}'_u$  is, in general, variable depending on  $\hat{\nu}_u$ ,  $\hat{\nu}_m$ , and  $\phi$ . The angular dependence in this equation is a consequence of the fact that self-consistent application of Maxwell's equations<sup>47</sup> for the plasma conditions of interest shows that the perturbation amplitude  $\vec{E}_k$  is aligned with the wave vector  $\vec{k}$ , while  $\vec{J}_k$  is perpendicular to  $\vec{k}$ . Thus the first-order perturbation in the electron joule heating,  $\vec{J}_{e_k} \cdot \vec{E} + \vec{J}_e \cdot \vec{E}_k$ , exhibits a spatial dependence relative to the direction of the wave-propagation vector,<sup>7</sup> with the result that the relationship between disturbances in electron density and temperature is nonisotropic.

Equation (12) is valid when volume processes dominate electron energy exchange, even in the region of a small local disturbance. The characteristic time for electron energy transport into or out of the region of a disturbance of characteristic size  $k^{-1}$  is  $(v_d k)^{-1}$ , where  $v_d$  is the electron drift velocity. The relationship between  $T_{e_k}$  and  $n_{e_k}$  as expressed in Eq. (12) is therefore applicable as long as  $(v_d k / \nu_u) \ll 1$ , implying that the influence of electron energy transport in the local region of a disturbance is insignificant compared to electron energy loss due to collisions. In molecular gas discharges at pressures above approximately 10 Torr,  $(v_d k / \nu_u)$  is on the order of  $10^{-2}$  or less for a  $k^{-1}$  value of 1 cm. For this reason the coefficient coupling the amplitudes of electron temperature and density perturbations is *real*<sup>7,48</sup> when collision processes dominate plasma behavior, indicating that disturbances in these

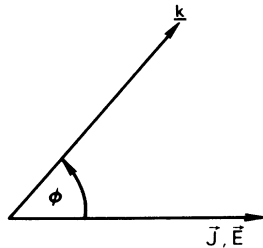


FIG. 6. Spatial relationship between the direction of the unperturbed current density and electric field vectors and the wave-propagation vector  $\vec{k}$ .

electron properties are locked in phase at either  $0^\circ$  or  $180^\circ$ , depending on the sign of  $\hat{\nu}'_u$ .

#### B. Temporal sequence of events accompanying disturbance

Equation (12) reveals two important properties of the response of the plasma to a disturbance. First, the quasisteady energy kinetics leading to the initial coupling between disturbances in electron temperature and electron density is spatially dependent relative to the direction of the wave vector  $\vec{k}$ ; second, the nature of the coupling between  $T_{e_k}$  and  $n_{e_k}$  depends on the relative strength of the electron temperature dependences of electron energy exchange and momentum-transfer collision processes, i.e., on the sign of  $\hat{\nu}'_u$ . The importance of the electron temperature dependence of  $\nu_u$  is obvious from the form of Eq. (10), while the role of the electron temperature dependence of  $\nu_m$  results from the fact that the electron current density depends on the momentum-transfer collision frequency.<sup>7,49</sup> Thus, since  $\nu_u$  and  $\nu_m$  vary significantly from species to species, both the magnitude and sign of  $\hat{\nu}'_u$  are in general variable. However, reliable data exist for  $\nu_u$  and  $\nu_m$  for the species of present interest.<sup>49</sup> These data show that, except in very unusual cases, the electron temperature dependence of the energy exchange collision frequency  $\nu_u$  is positive and is stronger than that of the momentum transfer collision frequency  $\nu_m$ . This implies that although the quantity  $1 + \hat{\nu}_u - \hat{\nu}_m \cos 2\phi = \hat{\nu}'_u$  depends on a spatial orientation,  $\hat{\nu}'_u$  is almost always positive, i.e.,  $1 + \hat{\nu}_u > \hat{\nu}_m$ . Numerical analysis of a wide variety of gas mixtures and electron temperature ranges typical of glow discharges shows that the magnitude of  $\hat{\nu}'_u$  is usually in the range 1–5. Thus, in addition to indicating that disturbances in electron temperature and electron density are strongly coupled only *along* the direction of the steady field and current, since  $\hat{\nu}'_u$  is generally a positive quantity of order unity, Eq. (12) also indicates that in volume-dominated plasmas  $T_{e_k}$  and  $n_{e_k}$  are usually  $180^\circ$  out of phase.

The entire coefficient,  $-2 \cos^2 \phi / \hat{\nu}'_u$ , relating the perturbation amplitudes  $T_{e_k}$  and  $n_{e_k}$  has been computed for a  $\text{CO}_2\text{-N}_2\text{-H}_2$  mixture as a function of angle and is presented in Fig. 7 for two values of electron temperature. In the direction of  $\vec{J}_e$  and  $\vec{E}$  ( $\phi = 0$ ), the coefficient coupling  $T_{e_k}$  and  $n_{e_k}$  is negative for the reasons cited previously, and is of order unity for both values of electron temperature. This result is found to be relatively insensitive to variations in electron temperature and/or gas mixture. In fact, the mixture and electron temperature values used in the examples presented in Fig. 7 correspond to an unusually wide variation

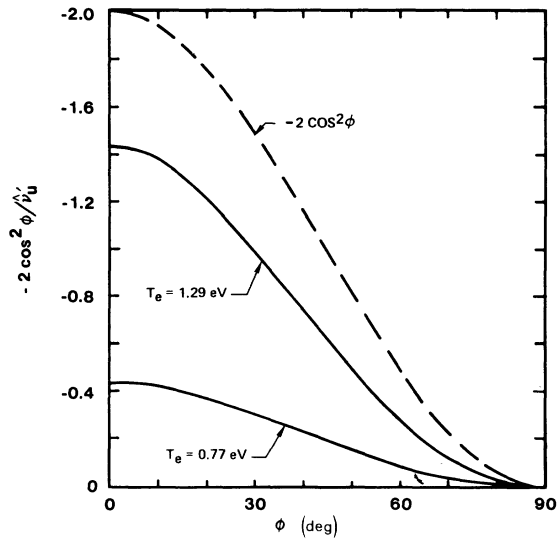


FIG. 7. Coefficient relating the quasisteady perturbation amplitudes  $T_{e_k}$  and  $n_{e_k}$  computed for the  $\text{CO}_2$  mixture and conditions of Fig. 5. For comparison, the quantity  $-2 \cos^2 \phi$  which corresponds to the situation for which the electron energy exchange and momentum-transfer collision frequencies are independent of electron temperature is also shown.

in the magnitude of  $\hat{v}'_u$ . Therefore it can be concluded that in a large majority of cases a positive local disturbance in electron density is *initially* accompanied by a decrease in electron temperature in volume-dominated molecular gases because of the quasisteady nature of the electron energy response and the typical relationship between the electron temperature dependences of the electron energy exchange and momentum-transfer collision frequencies. This is a very important but frequently overlooked result, the consequences of which will now be examined.

#### 1. Charged particle production and loss instability—no negative ions

In order to appreciate the implications of the previous discussion it is worthwhile to first examine the time-dependent *response* of electron production and loss processes in the *absence* of negative-ion effects. If temporal amplification of an initial disturbance in electron density occurs, an instability in the electron production and loss processes will result. Throughout the remainder of the present paper this mode of unstable behavior will be referred to as *ionization instability*. The possible occurrence of ionization instability in recombination-dominated discharges can be readily assessed by examining the first-order perturbation of the electron continuity equation [Eq. (1)], neglecting terms involving the negative ions. In

this case it is easily shown that the perturbed form of Eq. (1) in the absence of external ionization is given by the relation

$$\frac{n_{e_k}}{n_e} \text{Re}(i\omega) = -n_e k_r^e \frac{n_{e_k}}{n_e} + nk_i \hat{k}_i \frac{T_{e_k}}{T_e}, \quad (13)$$

where the electron temperature dependence of the recombination coefficient has been neglected relative to that of the ionization coefficient since  $\hat{k}_r^e \ll \hat{k}_i$ . Equation (12) can now be used to eliminate the perturbation amplitudes  $T_{e_k}$  and  $n_{e_k}$  from Eq. (13), resulting in a simple expression for the disturbance growth rate,  $\text{Re}(i\omega)$ . The following criterion for ionization *instability* in a recombination-dominated plasma is obtained:

$$\text{Re}(i\omega) = nk_i \left( \frac{-2 \cos^2 \phi}{\hat{v}'_u} \hat{k}_i - 1 \right) > 0. \quad (14)$$

Examination of the form of Eqs. (12) and (13) shows that in this inequality the first term in the parentheses is a measure of the effect of a perturbation in electron temperature. Since  $\hat{k}_i > 0$ , reflecting the strong increase in the electron production rate with increasing electron temperature (Fig. 1), and since  $\hat{v}'_u > 0$  for the reasons discussed previously, the first term in Eq. (14) is always negative, i.e., stabilizing. The 1 appearing in Eq. (14) occurs because the exponent of the electron density in the electron-ion recombination term [ $n_e^2 k_r^e$  in Eq. (1)] is one higher than that of the direct ionization term [ $n_e nk_i$  in Eq. (1)]. Thus, because the *direct* electron density dependence of the recombination process is stronger than that of single-step ionization, recombination always exerts a stabilizing influence (see also the Appendix). Clearly then, the effect of disturbances in both electron temperature and electron density exerts a stabilizing influence in this example; viz., the inequality in Eq. (14) cannot be satisfied. The reason for this result is that when direct ionization and recombination dominate electron production and loss, a small time-dependent increase in electron temperature tends to be accompanied by an increase in electron density. This does not re-enforce the quasisteady relationship *initially* established between the perturbations in electron density and temperature resulting from the fast response of the electron energy exchange processes [Eq. (12)]. To further illustrate this effect the sequence of events accompanying a small disturbance in electron density in this limit is depicted by the diagram in Fig. 8(a). For ionization instability to occur a positive feedback mechanism at the collisional level-coupling electron production *and* energy kinetics is required. When attachment and detachment processes are important such an eventuality becomes possible [Fig. 8(b)]

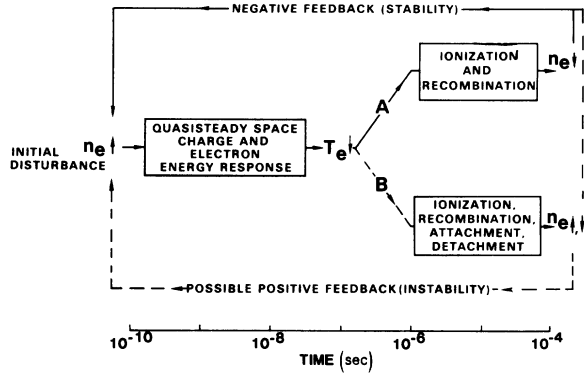


FIG. 8. Diagrammatic illustration of the sequence of events following an initial disturbance in electron density: A, when ionization and recombination dominate electron production and loss, and B, when attachment and detachment processes are also important. The accompanying time scale provides an approximate measure of the characteristic response time of the indicated processes for the discharge conditions of primary interest.

for reasons which will become apparent from the discussion to follow.

## 2. Charged-particle production and loss instability—negative ions present

When the negative-ion processes *are* important, the first-order electron production and loss equation is considerably more complicated than in the case of the simple situation discussed above relative to Eq. (13). Perturbations in the negative-ion concentration must now be taken into account, re-

quiring consideration of Eq. (3). Thus, because of the influence of attachment and detachment it is no longer clear whether a temporal increase or decrease in electron density will occur in response to an initial perturbation in electron temperature. Furthermore, disturbances in electron density and negative-ion density develop in approximately the same time range, so that retention of both time derivatives in the perturbed forms of Eqs. (1) and (3) results in a quadratic equation for  $\omega$ . One root of this equation is identifiable with the mode of instability associated with the electron production and loss process (ionization mode) as discussed previously, while the other is associated with the production and loss of negative ions (negative-ion mode). The two roots of the quadratic equation of interest can of course be expressed in the form

$$\text{Re}(i\omega_\alpha) = \frac{1}{2}(-b) \pm \frac{1}{2}(b^2 - 4c)^{1/2}, \quad (15)$$

where the quantities  $b$  and  $c$  are *real* functions of the steady-state properties of the plasma. The plus and minus signs before the radical in Eq. (15) do not distinguish between the ionization and negative-ion modes of instability. Although not readily apparent, which sign corresponds to the ionization mode, for example, depends on the relationship between the signs of  $b$  and  $c$ . The relationship between the signs of these coefficients and the two modes of instability will be discussed in subsequent paragraphs.

The coefficients  $b$  and  $c$  have been derived by Haas<sup>7</sup> and are given by the equations

$$b = nk_i \hat{k}_i \left( \frac{2 \cos^2 \phi}{\hat{v}_u'} \right) \left( 1 - \frac{k_a \hat{k}_a}{k_i \hat{k}_i} \right) + \left( \frac{n_e n_p k_r^e}{n_p} + \frac{n_n nk_a}{n_e} + \frac{n_n n_p k_r^i}{n_p} + \frac{n_e nk_a}{n_n} + \frac{n}{n_e} S \right), \quad (16)$$

$$c = nk_i \hat{k}_i \left( \frac{2 \cos^2 \phi}{\hat{v}_u'} \right) \left\{ \left( \frac{n_n n_p k_r^i}{n_p} + \frac{n_e nk_a}{n_n} \right) - \left[ \left( 1 + \frac{n_n}{n_p} \right) n_p k_r^i + \frac{n_e n_p k_r^e}{n_p} \right] \frac{k_a \hat{k}_a}{k_i \hat{k}_i} \right\} + \left[ \frac{n_e nk_a n_p k_r^e}{n} + \frac{n_n n_p k_r^i nk_a}{n_e} + \left( \frac{n_n n_p k_r^i}{n_p} + \frac{n_e nk_a}{n_n} \right) \frac{n}{n_e} S \right]. \quad (17)$$

Clearly, considerable complication arises as a consequence of the coupling between electron and negative-ion production and loss processes. However, the complications are primarily algebraic and the influence of negative-ion processes on ionization instability is amenable to interpretation similar to that discussed in connection with Eq. (14) and Fig. 8(a).

Careful consideration of the various physical processes contributing to the terms in the coefficients  $b$  and  $c$  shows that when  $b$  is negative the ionization

mode will be unstable, and when  $b$  and  $c$  are of opposite sign the negative-ion mode will be unstable.<sup>7</sup> Thus in general the ionization and negative-ion modes can be unstable either individually or simultaneously. However, numerical evaluation of Eqs. (16) and (17) has shown that for the general conditions of interest  $c$  is always positive, while  $b$  changes sign. Therefore, with  $c > 0$  the negative-ion mode will be unstable only for those conditions such that the ionization mode is also unstable, i.e.  $b < 0$ . However, detailed analysis

(Ref. 7, Sec. IVD) of the physical processes involved in the coupling of these charged-particle modes of instability has shown that when the conditions for instability of the ionization and negative-ion modes are satisfied simultaneously, as in the cases of present interest, the former has the largest growth rate and therefore will evolve sufficiently rapidly to dominate plasma temporal behavior.<sup>7,46</sup> For this reason in the discussion to follow emphasis will be directed toward analysis of the factors influencing the ionization mode of instability. It should be pointed out that the purpose of the subsequent discussion is to determine and understand the nature of the unperturbed plasma conditions for which ionization instability is likely to occur, and by so doing to interpret the causes of instability in terms of basic collision phenomena occurring in the plasma as discussed in Sec. II.

### C. Attachment-induced ionization instability

The discussion in connection with Eqs. (13) and (14) and Fig. 8(a) indicated that a positive feedback mechanism coupling disturbances in electron energy density and particle conservation does not exist in recombination-dominated plasmas (except in the case of strong multistage ionization; see Appendix). Fortunately, assessing the impact of negative-ion processes on the stability of the electron production and loss processes does not require solution of Eqs. (15)–(17). Rather, for the reasons discussed above, analysis of the factors contributing to the sign of the coefficient  $b$  provides the needed information regarding electron production and loss instability. The occurrence of this mode of instability requires that  $b$  be negative. Thus the criterion for ionization instability when negative ions are present may be expressed

$$\left[ \left( \frac{-2 \cos^2 \phi}{\hat{v}'_u} \right) \left( 1 - \frac{k_a \hat{k}_a}{k_i \hat{k}_i} \right) n k_i \hat{k}_i \right] - \left( \frac{n_e}{n_p} n_p k_r^e + \frac{n_n}{n_e} n k_a + \frac{n_n}{n_p} n_p k_r^i + \frac{n_a}{n_n} n k_a + \frac{n}{n_e} S \right) > 0. \quad (18)$$

By omission of the terms involving negative-ion processes and by noting that in the absence of negative-ion effects  $n_e = n_p$  and  $n k_i = n_p k_r^e$ , it becomes clear that the criterion for instability expressed in Eq. (18) reduces to that in Eq. (14). Recall that examination of Eq. (14) indicated that when only direct electron-impact ionization and recombination processes are important ionization instability does not occur. Thus, the differences between Eqs. (14) and (18) reflect the important influence of negative-ion processes such as attach-

ment, detachment and negative-ion recombination on the stability of the electron production and loss process.

### 1. Necessary condition for instability

By direct analogy with Eq. (14), the bracketed group of terms in Eq. (18) represents the effect of changes in electron production and loss caused by a small amplitude disturbance in electron temperature; recall that the logarithmic derivatives  $\hat{k}_i$  and  $\hat{k}_a$  are a measure of the sensitivity of the ionization and attachment processes to variations in electron temperature. Thus the ratio  $k_a \hat{k}_a / k_i \hat{k}_i$  is simply  $\delta k_a / \delta k_i$ , the change in  $k_a$  associated with a change in  $k_i$  in response to a variation in electron temperature. The group of terms in parentheses reflects the direct coupled effect of disturbances in positive- and negative-ion density, and the stabilizing influence of an external ionization source. Disturbances in the positive-ion density and negative-ion density are controlled by electron-ion recombination and by negative-ion detachment, respectively. These processes exert a damping influence, recombination by reducing the magnitude of disturbances in electron density, and detachment by reducing the negative-ion concentration. For this reason all the components of the second grouping of terms are positive quantities. Therefore, the second group of terms, although of variable magnitude, exerts a stabilizing influence for all conditions and is analogous to the 1 in Eq. (14). Thus, it becomes clear that with  $\hat{v}'_u > 0$ , as is almost always the case, a necessary condition for ionization instability is that the quantity  $k_a \hat{k}_a / k_i \hat{k}_i$  exceeds unity. Practically, this requires (i) that the electron attachment coefficient be an increasing function of the electron temperature, and (ii) that the attachment coefficient be of a magnitude at least comparable to that of the ionization coefficient. When the quantity  $k_a \hat{k}_a / k_i \hat{k}_i$  exceeds unity, the loss of electrons resulting from electron-molecule attachment dominates over electron production from ionization during a positive fluctuation in electron temperature. The dominance of attachment over ionization during a disturbance favors an inverse relationship between disturbances in electron temperature and electron density, thereby *re-enforcing* the relationship between these quantities established by the instantaneous electron energy kinetics discussed previously in connection with Eq. (12). Such a positive feedback mechanism at the collisional level, as illustrated in Fig. 8(b), can lead to *electron-attachment-induced-ionization instability* when  $k_a \hat{k}_a / k_i \hat{k}_i > 1$ , if the effect of electron temperature disturbances is sufficient to overcome the damping influence of

recombination and detachment processes [second term in Eq. (18)]. Further, the angular variation of Eq. (18) shows that even with  $k_a \hat{k}_a / k_i \hat{k}_i > 1$  the necessary condition for this mode of instability can be satisfied only for values of  $\phi$  near zero; that is, in the direction of the unperturbed electric field. Wave growth in the direction of the steady field is conducive to the formation of a layering in plasma properties ultimately leading to a striated plasma.

Examination of the ionization and attachment rate coefficients presented in Figs. 1 and 2 shows that for several species of interest such as  $\text{CO}_2$ ,  $\text{CO}$ , and  $\text{O}_2$ , the ionization and attachment coefficients are indeed of comparable magnitude for electron temperature values near 1 eV. Further, both the ionization and attachment coefficients for these species are strongly increasing functions of electron temperature. Computations for numerous experimentally interesting situations show that the condition  $k_a \hat{k}_a / k_i \hat{k}_i > 1$  is easily satisfied for electron temperature values of approximately 1 eV. Representative results are presented in Fig. 9. These data indicate that the quantity  $k_a \hat{k}_a / k_i \hat{k}_i$  is itself a very strong function of electron temperature, changing in magnitude by a factor of approximately 100 for relatively small changes in electron temperature. More importantly, with  $k_a \hat{k}_a / k_i \hat{k}_i$  exceeding unity for electron temperature values of about 1 eV, it becomes clear that for conditions typical of electric discharges attachment can dominate over ionization during a disturbance in electron temperature, thereby satisfying the necessary condition for attachment-induced ionization instability.

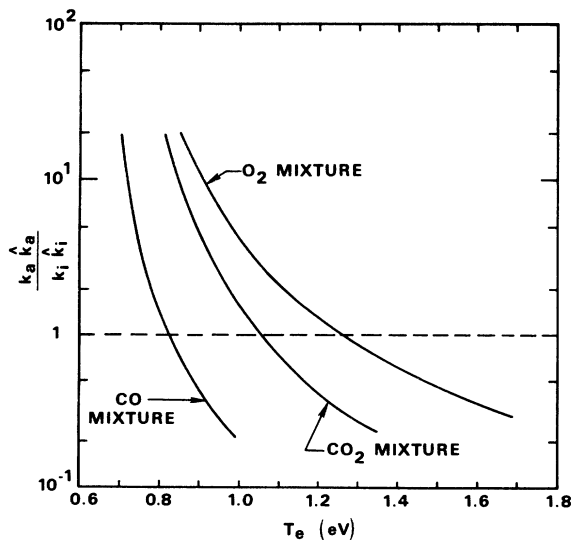


FIG. 9. Computed electron temperature dependence of the quantity  $k_a \hat{k}_a / k_i \hat{k}_i$  for  $X\text{-N}_2\text{-He}$  (0.05:0.35:0.60) gas mixtures, where  $X = \text{CO}_2$ ,  $\text{O}_2$ , or  $\text{CO}$ .

## 2. Sufficient conditions—self-sustained discharges

For the effect of negative-ion production (electron loss) during an electron temperature disturbance to exceed the stabilizing influence of recombination and detachment [second term in Eq. (18)] resulting in the positive feedback required for attachment-induced ionization instability, the net effect of negative-ion production and loss processes must be such that the negative-ion concentration is of approximately the same magnitude as that of the electrons. When this situation occurs electron and negative-ion processes can couple during a disturbance in plasma properties, leading to attachment-induced ionization instability.

If the negative-ion density is very low because of the stabilizing influence of detachment (discharge operation at point  $b$ , Fig. 4) the characteristic time for the negative ions to respond to a disturbance,  $(nk_a)^{-1}$ , is very much less than the time required for the electron density to respond. In this limit negative-ion processes respond in a quasisteady fashion as compared to the finite temporal response of the electron density during a disturbance. Thus, when the detachment is very effective, with the result that  $n_n/n_e \ll 1$ , negative-ion processes have no influence on either steady-state or transient electron production and loss processes, independent of the value of  $k_a \hat{k}_a / k_i \hat{k}_i$ . Even though  $k_a \hat{k}_a / k_i \hat{k}_i$  may be much larger than unity, a large detachment rate can instantaneously free electrons from negative ions so that the net effect of negative-ion production and loss processes is entirely insignificant, and both the steady-state and transient behaviors are typical of a recombination-dominated plasma. By way of contrast, if detachment is unimportant (discharge operation at point  $a$ , Fig. 4) corresponding to the condition  $n_n/n_e \gg 1$ , so that ionization balances the entire electron loss due to attachment in the steady state, then  $k_a \hat{k}_a / k_i \hat{k}_i = \hat{k}_a / \hat{k}_i$ . In this limit of an attachment-controlled plasma, attachment-induced ionization instability requires an attachment rate which has a stronger electron temperature dependence than the ionization rate, i.e.,  $\hat{k}_a / \hat{k}_i > 1$ . As is apparent from the examples shown in Figs. 1 and 2, such a situation is unlikely indeed. Thus, the range of electron temperature values between points  $a$  and  $b$  in Fig. 4 is the most likely for the occurrence of ionization stability driven by the attachment process. In this region the characteristic production times of electrons and negative ions are of comparable magnitude corresponding to conditions for which the ratio  $n_n/n_e$  is approximately of the order of unity.

### 3. Numerical evaluation—self-sustained discharges

In order to evaluate the stability criterion expressed in Eq. (18), the steady or unperturbed relationships among electron density, negative-ion density, and electron temperature must be determined in a fashion which assures internal self-consistency with the theoretical stability criterion itself. This is of considerable importance since each of the individual terms contributing to Eq. (18) has a magnitude much larger than the sum of all the terms.<sup>42</sup> This is almost always the case so that use of merely *reasonable* or *plausible* values of plasma properties to evaluate the terms contributing to the inequality expressed in Eq. (18) is of little value, and can actually be very misleading. While one can never be sure that all important processes have been included in the formulation, satisfying self-consistency is possible if the time-independent conservation equations (1) and (3) are numerically evaluated to determine a self-consistent relationship between electron temperature and the charged-particle densities. In addition, all the electron rate coefficients and  $\hat{k}$  quantities must be evaluated in the same manner. With this in mind the stability criterion expressed in Eq. (18) was evaluated taking the electron density and CO fractional concentration as variable parameters. This procedure permitted establishment of an ionization instability boundary as a function of both current density (electron density) and concentration of a typical additive which detaches electrons from  $O^-$ , the *initial* negative-ion species. Results of representative calculations in which  $CO_2$  and  $O_2$  provide the  $O^-$  are presented in Figs. 10 and 11. The shaded area of these figures indicates the region within which the criterion for *instability* expressed in Eq. (18) was found to be satisfied. Thus, for plasma conditions typical of the shaded regions, a steady uniform plasma should not exist owing to the appearance of the attachment-induced ionization instability. As mentioned previously, within the unstable region,<sup>50</sup> the negative-ion mode is also computed to be unstable [ $b$  and  $c$  opposite sign, Eqs. (16) and (17)], but the growth rate corresponding to this unstable mode is found to be substantially less than that of the ionization mode throughout most of the region. Thus, for the reasons elaborated upon by Haas<sup>7</sup> and by Rognlien and Self,<sup>46</sup> the ionization mode should dominate plasma temporal behavior. Similar calculations made with CO as the source of negative ions revealed very low negative-ion concentrations and no region of instability, although Fig. 9 indicates that the *necessary* condition for instability can be satisfied for

the CO mixture. This result is to be expected since CO itself is the primary detaching species under consideration.

The variation of the computed stability boundaries shown in Figs. 10 and 11 illustrates the dependence of the instability criterion on the steady values of electron temperature and negative-ion concentration. The minimum ratio  $n_n/n_e$  corresponding to the lower portion of the boundary is approximately 0.1, below which ionization and recombination dominate plasma behavior. While the upper portion of the boundary corresponds to very high relative negative-ion concentrations  $n_n/n_e > 1$ , and the plasma behavior is attachment controlled,<sup>38</sup> the electron temperature value required to compensate for the greater loss of electrons due to attachment corresponds to a condition for which  $k_a \hat{k}_a / k_i \hat{k}_i$  is below unity, so that the necessary condition for instability is not satisfied even though the negative-ion concentration is very high. Therefore it

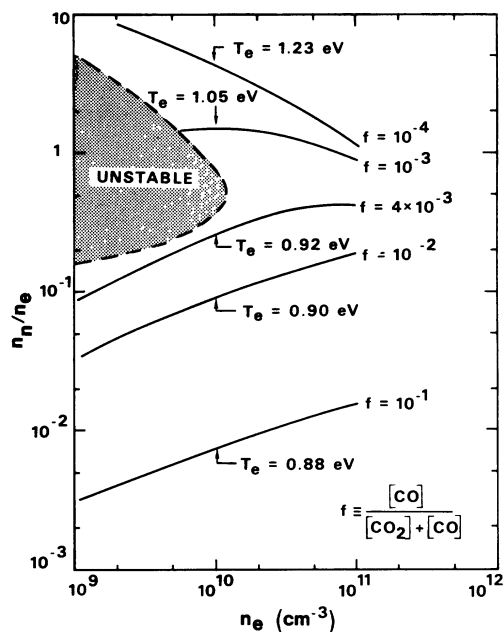


FIG. 10. Ionization instability boundary computed for a 20-Torr  $CO_2$ - $N_2$ -He mixture in the number density proportions 0.05:0.35:0.60. The electron density and CO fraction were taken as variable parameters in the calculation, and the negative-ion density, electron temperature, and stability criterion were computed in a self-consistent fashion as discussed in the text. The electron temperature values shown correspond to an electron density of  $10^{10} \text{ cm}^{-3}$ . On the basis of the present ionization instability model, a stable uniform plasma having the properties indicated in the figure can only exist exterior to the shaded region. As the instability boundary is crossed the analysis indicates that disturbances in the electron production-loss process will grow in time, indicative of ionization instability.



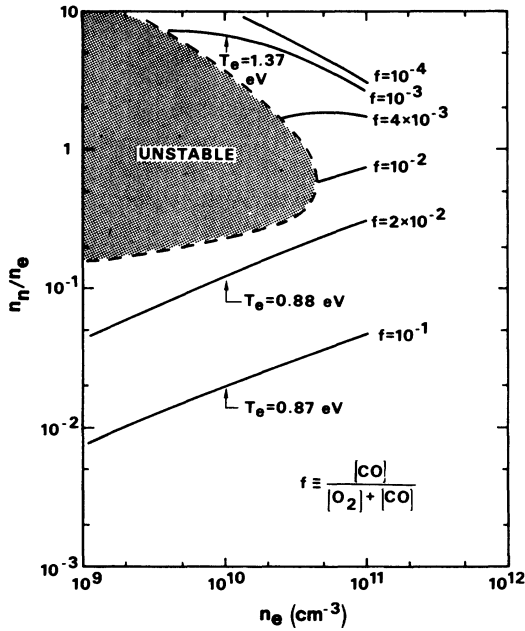


FIG. 11. Ionization instability boundary computed for an  $O_2$ - $N_2$ -He mixture in the number density proportions 0.05:0.35:0.60. The other conditions and interpretations are the same as those of Fig. 10.

becomes clear that the mere presence of large negative-ion concentrations does not necessarily lead to this mode of ionization instability. Rather, the critical factor is the net effect of negative-ion formation on electron production and loss during a disturbance in plasma properties.

#### 4. External ionization

When an external source of ionization is utilized to sustain a plasma, the applied electric field can be set arbitrarily, but is generally chosen such that the value of  $E/n$  (electron temperature) is well below that characteristic of point  $a$  in Fig. 4. Thus the contribution to the ionization rate due to the drifting electrons is usually entirely negligible compared with that provided by the external source. If conditions are such that detachment is also unimportant, examination of Fig. 4 reveals a rather broad range of electron temperature values (between points  $a$  and  $c$ ) for which attachment rather than recombination is the dominant electron loss process. By omitting the terms involving electron recombination, ionization, and detachment in Eq. (18), a simplified criterion for ionization instability appropriate to an externally maintained plasma can be obtained:

$$nk_a \left[ \frac{2 \cos^2 \phi}{\hat{v}'_u} \hat{k}_a - \left( 1 + \frac{n_e}{n_p} + \frac{n_e}{n_n} \right) \right] > 0. \quad (19)$$

Here use has been made of the steady-state relations  $n_e nk_a = nS = n_n n_p k_r^i$ . The assumptions made in arriving at Eq. (19) also imply that the ratios  $n_e/n_p$  and  $n_e/n_n$  are small, indicating that in this limit the criterion for ionization instability is readily satisfied whenever the attachment coefficient has a moderately strong positive electron temperature dependence, i.e.,  $\hat{k}_a \gtrsim 1$ . It should be noted that recombination and detachment processes frequently make important contributions when an external source of ionization is utilized, so that the more general criterion expressed in Eq. (18) has considerably broader applicability than Eq. (19).

Recently electron attachment-induced ionization instability was observed by Douglas-Hamilton and Mani<sup>51</sup> using  $CO_2$ -He and  $H_2O$ -He mixtures in an atmospheric-pressure electron-beam-sustained discharge. These investigators adopted the term *electron attachment* instability to describe the observed phenomenon, whereas, throughout the present investigation the general class of instability associated with the electron production and loss processes is referred to as *ionization-instability* regardless of the precise electron collisional processes causing its occurrence (see Appendix). Nevertheless, of considerable significance is the fact that the observations of Douglas-Hamilton and Mani using a discharge sustained by an external source of ionization provide strong corroborative evidence in support of the present interpretation of the influence of negative-ion processes on plasma stability.

#### IV. EXPERIMENTAL INVESTIGATIONS

The ranges of electron densities, electron temperatures, and negative-ion concentrations encompassed by the computed unstable regions shown in Figs. 10 and 11 suggest that conditions favoring ionization instability will frequently be encountered in laboratory discharges. In order to validate the essence of the present analytical results for *self-sustained* steady discharge conditions, experimentation was conducted using a cylindrical 3.8-cm-diam 70-cm-long convection-dominated discharge.<sup>52</sup> Investigations using  $CO_2$ - $N_2$ -He,  $CO$ - $N_2$ -He, and  $O_2$ - $N_2$ -He mixtures in the 10–50-Torr range were carried out. For a nominal value of flow velocity of 100 m/sec, the gas residence time in the discharge was less than  $10^{-2}$  sec, so that electron-impact dissociation of the initial molecular species had a minimal effect on the gas mixture. Further, for these conditions thermal conduction to the tube walls was entirely unimportant relative to energy removal by convection, with the result that gradients in medium properties were

very much less than would be the case in slowly flowing or sealed discharges. This is of some importance since the present theory is strictly applicable only for plasmas dominated by volume collision processes. When transport phenomena become important at least the quantitative interpretation of the results discussed in previous sections will be modified. In this investigation the experimental pressure range was selected to span the range of electron loss mechanisms from partial diffusion control to total volume loss domination.

#### A. Gas-mixture variations

The basic gas mixture utilized in the experimental studies was composed of  $X$ - $N_2$ -He in the number density proportions 0.05:0.35:0.60, where the species designated  $X$  is either CO,  $CO_2$ ,  $O_2$ , or combinations of these gases. For these mixtures, the test species  $X$  and the  $N_2$  make approximately equal contributions to the ionization rate. More importantly, for mixtures having these general proportions, the form of the electron energy distribution function is determined almost entirely by electron collisions with  $N_2$  owing to the relatively large nitrogen vibrational, electronic, and elastic cross sections. Hence by maintaining the concentration of the species  $X$  at a relatively low level compared with the  $N_2$  content, the impact of the various attachment, detachment, and negative-ion clustering processes specific to each negative-ion-producing species could be assessed without the additional discharge complications which might arise due to changes in the electron energy distribution function itself. The judicious addition of small quantities of CO as a detachment agent<sup>53</sup> permits the stability characteristics of discharges in these gas mixtures to be determined in a fashion directly comparable with the analytical data presented in Figs. 10 and 11. For the purposes of this comparison, the discharge electron density can be determined from a knowledge of the current density,  $E/n$  ratio, and electron drift velocity computed for the mixture.<sup>11,12</sup> Since electron drift velocity can be computed with an accuracy of approximately  $\pm 20\%$ , electron density values determined in this manner are felt to be more reliable than those determined by most available experimental methods.

#### B. Experimental results

##### 1. Qualitative observations

For typical experimental conditions the discharges for all mixtures were well behaved and appeared to be uniform to the naked eye. However, oscilloscope monitoring of the plasma potential

variations measured using electrostatic probes, and display of the sidelight fluctuations as detected by a photomultiplier, revealed that the discharges in the  $CO_2$  and  $O_2$  mixtures were in fact striated, a result compatible with wave growth along the direction of current flow,  $\phi = 0^\circ$ . Representative voltage, electric field, and sidelight fluctuations associated with these running striations are shown in Fig. 12. Upon the addition of carbon monoxide to these mixtures in increasing amounts, the magnitudes of the measured fluctuations were observed to decrease smoothly toward zero and the applied discharge voltage at constant current was found to increase asymptotically to a higher value.<sup>54</sup> When sufficient  $CO$ <sup>53</sup> was titrated into these discharges the striations were found to be completely suppressed, presumably due to the rapid detachment of electrons from the negative ion  $O^-$ . When CO alone was used as the species  $X$ , no striations were ever observed, again owing to the rapid associative detachment reaction. These findings are in very good qualitative agreement with the theoretically predicted behavior discussed in previous sections.

##### 2. Diagnostic methods

In order to evaluate the theoretical stability boundary in a more quantitative fashion, the fractional concentration of CO required to remove running striations from the mixtures containing  $CO_2$  and/or  $O_2$  was carefully measured. Because

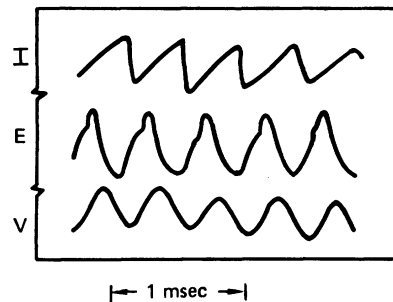


FIG. 12. Tracings of oscilloscope photographs of fluctuations in voltage, electric field, and sidelight intensity associated with the occurrence of striations in mixtures containing  $CO_2$  or  $O_2$ . The voltage fluctuations were detected on one of the several electrostatic probes positioned at the wall along the length of the column from which the static electric field was also determined. The fluctuation in electric field was obtained by electronically differentiating the voltage signal. Sidelight emission from the  $N_2$  second positive system ( $\lambda \sim 3755 \text{ \AA}$ ) was observed with a photomultiplier and a bandpass filter. The phase difference between voltage and light fluctuation is of no significance since the points of observation were not coincident.

of the gradual disappearance of the striations with the increasing CO content, the assignment of the value of CO fraction  $f$  corresponding to suppression of the instability was somewhat arbitrary. For this reason a spectrum analyzer was utilized to display the magnitude of the voltage fluctuation at the fundamental striation frequency ( $\sim 5$  kHz); when the voltage fluctuation became small compared with the normal discharge background noise, the striations were determined to have been removed and the *critical* CO fractions  $f_c$  noted. This method of determining the value of CO fraction required to remove striations was applied uniformly for all the measurements. However, simultaneous observation of the increase of the average discharge voltage toward its unstriated value suggested that this definition may have been somewhat conservative, in that the voltage asymptotically reached its saturated value before the fluctuations were fully suppressed. For this reason the measured value  $f_c$  is consid-

ered to be uncertain by approximately a factor of 2. However, the theoretical data plotted in Figs. 10 and 11 indicate that changes in  $f$  of a factor of 2 are relatively unimportant considering the range of  $f$  values required to span the unstable region. Thus, the method of establishing the stability boundary based on titrating CO into the gas mixture provides the most direct and unambiguous quantitative comparison between theory and experiment.

Several additional features of these measurements should be noted. (a) The very low CO (or, equivalently, O) content corresponding to the upper portion of the computed unstable regions in Figs. 10 and 11 is below that normally produced in the discharge by electron dissociation of the  $\text{CO}_2$  (Fig. 3) and/or  $\text{O}_2$ . Thus, the very low concentrations of detaching species determining the upper portion of the stability boundary were not accessible for conditions typical of the steady-state experiments under study. (b) Even for the values of  $f$  computed to lie within the midportion of the unstable region, increasing the electron density actually results in a change in the detaching species since  $\text{CO}_2$  and  $\text{O}_2$  dissociation increases with electron density. However, the value of  $f$  corresponding to the *lower* portion of the computed stability boundary in Figs. 10 and 11 is nearly constant and, more importantly, is high enough to be relatively unaffected by the naturally occurring CO and/or O formation in the discharge. Therefore, the measurement of the critical CO concentration ( $f_c$ ) which must be added to the mixture in order to *suppress* striations is a simple and useful diagnostic which permits convenient comparison of experiment with theory.

### 3. Critical CO fraction

Figure 13 presents the measured critical CO fractions for an X- $\text{N}_2$ -He mixture in the proportions 0.05:0.35:0.60, where X represents the combined  $\text{CO}_2$  and  $\text{O}_2$  fractional densities at a constant value of 0.05. Also shown in the figure is a solid line approximating the lower portion of the computed stability boundary for these mixtures, as determined from the data of Figs. 10 and 11. Recall that in the analytical model the initially produced negative ion  $\text{O}^-$  is assumed to be lost *only* by detachment and positive-ion-negative-ion recombination. For the reasons cited previously in connection with the discussion of Fig. 5, this assumption is reasonable for the  $\text{O}_2$  mixture in the presence of small amounts of CO, since for CO concentrations corresponding to  $f$  values above  $10^{-3}$  the  $\text{CO-O}^-$  detachment reaction readily competes with the cluster reaction  $\text{O}^- + \text{O}_2 + M \rightarrow \text{O}_3^- + M$ . Thus the value  $f_c$  defining the lower portion of the

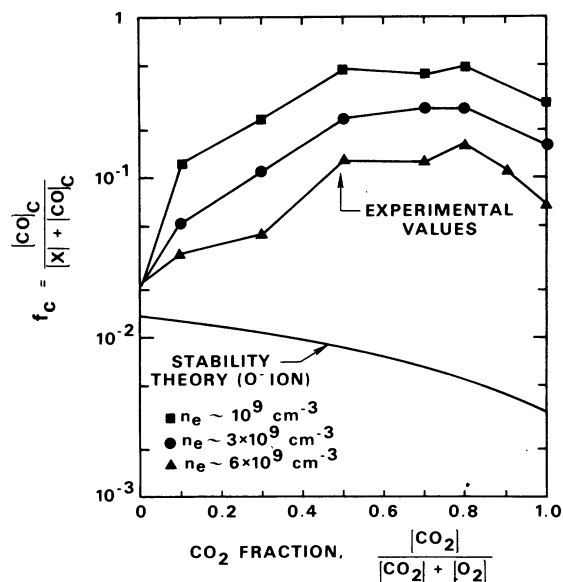


FIG. 13. Comparison of measured and computed fractional CO concentration required to *eliminate* striations from mixtures containing  $\text{O}_2$  and  $\text{CO}_2$  as described in the text. The gas pressure was 20 Torr with the mixture proportions X- $\text{N}_2$ -He (0.05:0.35:0.60), where X corresponds to the combined fractional concentration of  $\text{O}_2$  and  $\text{CO}_2$ . The theoretical curve in the absence of  $\text{CO}_2$  and  $\text{O}_2$  (left- and right-hand boundaries) corresponds approximately to the lower portion of the instability boundaries as shown in Figs. 10 and 11. As is the case for the data shown in Figs. 10 and 11, the lower portion of the stability boundary computed for mixtures containing both  $\text{CO}_2$  and  $\text{O}_2$  was also found to be relatively insensitive to electron density changes and therefore the theoretical curve in this figure is sensibly independent of electron density.

theoretical stability boundary for the  $O_2$  mixture (Fig. 11) is expected to be reasonably quantitative. The data of Fig. 13 indicate that such is indeed the case, with the difference between theory and experiment of approximately 50% falling well within the range of experimental and analytical uncertainty. However, as the transition is made from the  $O_2$  mixture to the  $CO_2$  mixture, the quantitative difference between theory and experiment increases substantially, with the experimentally determined  $f_c$  reaching a value of nearly 100 times the computed value at the lowest electron density value shown. Thus, when  $CO_2$  is the source of  $O^-$  it requires about 100 times more CO to remove striations than is predicted on the basis of a simple  $O^-$  attachment-detachment model.

The trend exhibited by the data of Fig. 13 can be explained on the basis of the negative-ion detachment and clustering kinetics appropriate to  $CO_2$  discharges. The clustering reaction  $O^- + CO_2 + M \rightarrow CO_3^- + M$  occurs approximately 300 times faster than the corresponding  $O_2$  reaction and, for the present conditions, is nearly 100 times faster than the CO detachment reaction for the computed value of  $f_c$ . Further, it is known<sup>34</sup> that CO does not detach electrons from  $CO_3^-$ . Thus, in contrast to the situation typical of the  $O_2$  mixture,  $O^-$  can be very rapidly converted to the permanent negative ion  $CO_3^-$  in the  $CO_2$  mixture. As the results of Figs. 10 and 11 indicate, the lower portion of the stability boundary (onset of striations) corresponds to conditions such that the negative-ion density is relatively small, i.e.,  $n_n/n_e \sim 0.2$ . In order to reduce the relative negative-ion concentration to this level in the presence of the fast  $CO_2$  clustering reaction, the CO density must be increased until electrons can be removed from  $O^-$  in associative detachment reactions *before* they can become permanently attached to form a  $CO_3^-$  ion. The comparative rate coefficients for the competing detachment and clustering processes suggest that values of  $f_c$  on the order of hundreds of times that expected from the simple  $O^-$  attachment-detachment model could be required, depending on the relative  $O^-$  and  $CO_3^-$  concentrations under specific discharge conditions. For these reasons the differences between the theoretical and experimental data shown in Fig. 13 for the  $CO_2$  mixture are felt to be understood and amenable to interpretation on the basis of present understanding of the processes involved. Unfortunately, the principal mechanisms by which the cluster negative ions such as  $CO_3^-$  and  $O_3^-$  are destroyed in active gas discharges are not fully understood at present, so that the systematic difference between theory and experiment cannot be accounted for by simply modifying the stability analysis to include the

effect of another species of negative ion. Nevertheless, it should be pointed out that the basic cause of instability is the same for both the  $CO_2$  and  $O_2$  mixtures, as discussed in connection with the theoretical data of Figs. 10 and 11. Further, the experimental observations of striations in both mixtures are essentially the same. Thus the clustering reactions affect specific details but not the essence of the attachment-induced instability.

In addition to the general variations between the theoretical and experimental values of the critical CO fraction, the data of Fig. 13 also show that the experimental values depend significantly on electron density (discharge current density). Increasing electron density results in an increase in gas temperature and a very large increase in the density of vibrationally excited molecules, two factors which are likely to influence the nature and density of the negative ions. Resolution of the role of these effects as regards  $CO_3^-$  and perhaps  $O^-$  loss processes<sup>55</sup> in discharges clearly requires additional basic data.

#### 4. $O_2$ discharges

In addition to the studies described above, preliminary investigations of the behavior of  $O_2$  discharges have been conducted. These limited observations were motivated by the reported differences in properties associated with the well-known "T" (striated, low average electric field) and "H" (unstriated, high electric field) forms of the oxygen discharge.<sup>42-44,56</sup> The titration of CO into striated  $O_2$ -He discharges operating at approximately 20 Torr removed the striations in all cases and resulted in increases of discharge voltage.<sup>54</sup> These findings indicate that the T form of the  $O_2$  discharge is a manifestation of the presence of the ionization instability caused by the electron attachment process forming  $O^-$  from  $O_2$ , as described previously. The naturally occurring transition from T to H discharge behavior observed previously is most likely caused by accumulation of a sufficient concentration of the detacher O [or perhaps  $O_2(a^1\Delta_g)$ ] in the gas mixture. Although previous investigators have suggested that negative ions were responsible in some way for the peculiarities of  $O_2$  discharges, none but Sabadil<sup>43</sup> has proposed a fundamental mechanism to explain the observed behavior. Sabadil's Gunn-instability analogy is similar in some respects to the electron attachment-induced instability mechanism described in the present paper.

#### V. SUMMARY

The objective of the present investigation has been twofold: First, to assess the impact of the

presence of negative ions on the basic plasma and collision processes occurring in weakly ionized volume-dominated discharges; second, to understand and explain the mechanisms by which basic processes involving negative ions affect the stability of charged-particle production and loss. The analytical results presented herein show how and why the details of attachment, detachment, and clustering processes exert such an important influence on *both* steady-state and transient plasma behavior. Further, experimental data reported herein and those obtained by other investigators<sup>38,51,54</sup> validate the essential aspects of the present theoretical analysis and interpretation over a wide variety of discharge conditions.

Analysis of charged-particle production and loss processes when negative ions are present indicates that the electron temperature value required to sustain a plasma can vary by almost a factor of 2 depending on whether the principal electron loss process is attachment or recombination. Further, it has been shown that modes of instability associated with electron production and loss (ionization instability), and negative-ion production and loss (negative-ion instability) can occur for easily attainable discharge conditions. Electron attachment-induced ionization instability has the largest growth rate of the two modes and will therefore dominate plasma temporal behavior, ultimately leading to a striated plasma. This mode of instability *can* occur when the magnitude of the electron attachment coefficient exceeds the ionization coefficient and has a comparable electron temperature dependence. Given this situation, instability *will* occur when negative-ion loss processes are such as to result in negative-ion concentrations comparable to the electron concentration. In this connection, clustering reactions involving the initial species of negative ion and its parent molecule have been shown to play an important role in establishing the steady negative-ion concentration. Thus both the steady-state value of electron temperature and onset conditions for instability are affected by processes involving the formation of clustered negative ions. However, present understanding of the mechanisms by which cluster negative ions are destroyed in active discharges is incomplete. Thus results of this investigation point out a need for additional data on cluster ion production and loss.

It should be mentioned that the causes of charged-particle production instability leading to the commonly observed striated discharge are, in general, extraordinarily complex and vary greatly as gas species and plasma operating conditions are changed. Therefore it is important to reiterate that the results and conclusions of the present

work, while applicable for a broad range of molecular gas discharge conditions, are not applicable for *all* situations. Although the assumptions discussed in Sec. II and elaborated in Sec. III are not unduly restrictive, the present treatment is limited to electrically excited molecular gas discharges which are dominated by volume phenomena, with transport processes playing only a minor role.

#### ACKNOWLEDGMENTS

The authors are pleased to acknowledge the helpful and stimulating comments of R. H. Bullis, R. A. Haas, and G. J. Schulz.

#### APPENDIX

In order to facilitate comparison of the present formulation and interpretation with the reported results of other investigators, it is worthwhile to comment briefly on two important aspects of glow discharge instability which do not fall within the intended scope of this paper.

##### A. Hydrodynamic stability model

The applicability of the quasisteady *hydrodynamic* description of electron energy relaxation during a disturbance, as described in Sec. III and Ref. 7, goes well beyond the requirement that the *average* energy relaxation time,  $\nu_u^{-1}(T_e)$ , be much less than the characteristic time for the electron density to change,  $[nk_i(T_e)]^{-1}$ . Rather, use of a hydrodynamic model requires that the response time of the electron energy distribution (for *all* values of electron energy) be much less than the electron production time. This condition can be easily satisfied *only* when inelastic collision processes such as vibrational excitation dominate the low-energy portion of the electron distribution function, *or* when values of fractional ionization are such that electron-electron collisions are effective in establishing and maintaining a nearly Maxwellian energy distribution. In weakly ionized noble gases, elastic energy losses often dominate the behavior of the body of the electron distribution and inelastic losses determine the form of the high-energy tail, with the result that the energy relaxation of the slow and fast electrons occurs on a very different time scale in response to a disturbance. Thus, although estimates of average electron properties may indicate that  $\nu_u \gg nk_i$ , the response of the electron energy distribution to a disturbance may not be quasisteady in its entirety. For conditions such that the relaxation of the electron energy distribution cannot be considered quasisteady, the linearized Boltzmann equation<sup>57-59</sup> must be solved in order to predict correctly the conditions for onset

of ionization instability, i.e., temporal growth of a disturbance in electron density. While experimentally observed dispersion characteristics of ionization waves in weakly ionized noble gases frequently can be predicted in a satisfactory fashion using a hydrodynamic model, the temporal response of the plasma to a perturbation cannot be predicted in accord with experimental observations without resorting to arbitrary variation of parameters or omission of important stabilizing terms in the electron energy equation, such as those descriptive of electron thermal conduction.<sup>42</sup> In this case analysis of the temporal response of the plasma when all unperturbed properties, transport coefficients, and rate coefficients are evaluated in a self-consistent fashion requires the considerable additional complexity introduced by use of the Boltzmann equation. Thus it is somewhat paradoxical that, for discharges in weakly ionized noble gases and other monatomic gases in which negative-ion and plasma chemical effects resulting from dissociation do not occur, a valid theoretical treatment is complicated by significant mathematical difficulties that are seldom required in the analysis of molecular gas discharges.

#### B. Multistage ionization

When the density of electronically excited species reaches the point where electron impact ionization from excited states becomes important, the stability of charged-particle production and loss processes can be dramatically altered. Since the production of excited species proceeds by way of electron impact and frequently is characterized by a time comparable to the ionization time, rigor requires that one or more additional time-dependent equations be taken into account, each corresponding to an additional root of the dispersion reaction, and therefore, another potential mode of instability. Clearly, complete analytical development in such circumstances can represent a formidable problem unless there is one dominant electronic level having well-known production and loss processes. However, certain of the more important implications of multistep ionization can be understood by observing that the primary influence of cumulative ionization is modification of the electron density dependence of the electron production process. In order to illustrate the potential significance of this effect on ionization instability, the ionization rate coefficient will be assumed to exhibit a dependence on *both* electron density<sup>42</sup> and electron temperature. The resulting first-order criterion for ionization instability in the absence of negative ions as expressed in Eq. (14) is modified in a simple but very important

way, i.e., for ionization instability

$$nk_i \left[ \left( \frac{-2 \cos^2 \phi}{\hat{v}'_u} \hat{k}_i \right) - \left( 1 - \frac{\partial \ln k_i}{\partial \ln n_e} \right) \right] > 0. \quad (\text{A1})$$

In this inequality the first term in parentheses is a measure of the effect of a perturbation in electron temperature, while the second term in parentheses reflects the influence of perturbations in electron *density*. In connection with the second term, the 1 appears in the first-order instability criterion since the exponent of the electron density in the electron-ion recombination term ( $n_e^2 k_r^e$ ) is one higher than that in the direct ionization term ( $n_e n k_i$ ). Thus, recombination exerts a stabilizing influence. When multistep ionization is considered as in the present approximation, the ionization rate coefficient  $k_i$  is assumed to exhibit a dependence on electron density, with the result that  $(\partial \ln k_i / \partial \ln n_e) > 0$ . As multistep ionization increases in importance, the magnitude of  $(\partial \ln k_i / \partial \ln n_e)$  increases, thereby offsetting the stabilizing influence of recombination.

Examination of the angular dependence of Eq. (A1) shows that, even when multistep ionization is sufficiently strong that the magnitude of  $(\partial \ln k_i / \partial \ln n_e)$  exceeds unity, the criterion for *instability* can be satisfied only for values of  $\phi$  near  $90^\circ$ . This conclusion follows from the observation that  $k_i \gg 1$ , and  $\hat{v}'_u$  is generally positive and of order one in collision-dominated plasmas for the reasons discussed in Sec. III. Disturbance growth in the direction perpendicular to the direction of the steady current density ( $\phi = 90^\circ$ ) is likely to favor filamentation of the plasma leading ultimately to constriction, in contrast to the striations resulting when disturbance growth occurs in the direction of the steady current, i.e.,  $\phi = 0^\circ$ . When the electron loss process depends on the first power of the electron density, as occurs when attachment dominates over recombination, the 1 does not appear in the second term of Eq. (A1), indicating that even very small amounts of multistep ionization may lead to disturbance growth for  $\phi = 90^\circ$ . While the analysis leading to Eq. (A1) and its subsequent interpretation are certainly qualitative, the potential significance of multistep electron production processes on the initial development and subsequent manifestation of ionization instability is apparent. Further, it becomes clear that the influence of cumulative ionization on discharge stability depends in an important way on the nature of the *other* electron production and loss processes. Thus, resolution of the role of multistep ionization on plasma stability requires careful consideration of the charged-particle kinetics processes in each specific situation.

- \*Work performed in part through the sponsorship of the Office of Naval Research and the Air Force Aerospace Research Laboratories and Air Force Weapons Laboratory, Air Force Systems Command, United States Air Force, under Contract No. F33615-73-C-4107.
- <sup>1</sup>K. G. Emeleus, E. W. Gray, J. R. M. Coulter, and G. A. Woolsey, *Intern. J. Electron.* **25**, 367 (1968).
  - <sup>2</sup>H. S. W. Massey, *Negative Ions* (Cambridge U. P., Cambridge, England, 1950), Chap. 5.
  - <sup>3</sup>K. G. Emeleus and G. A. Woolsey, *Discharges in Electronegative Gases* (Barnes and Noble, New York, 1970).
  - <sup>4</sup>D. Rapp and D. D. Briglia, *J. Chem. Phys.* **43**, 1480 (1965).
  - <sup>5</sup>W. L. Nighan, in *Proceedings of the Eleventh International Conference on Phenomena in Ionized Gases, 1973 (Invited Papers)*, edited by L. Pekárek and L. Láška (Czechoslovak Academy of Sciences, Prague, 1973), and references cited therein.
  - <sup>6</sup>A. E. Eckbreth and J. W. Davis, *Appl. Phys. Lett.* **21**, 25 (1972).
  - <sup>7</sup>R. A. Haas, *Phys. Rev. A* **8**, 1017 (1973).
  - <sup>8</sup>W. L. Nighan, W. J. Wiegand, and R. A. Haas, *Appl. Phys. Lett.* **22**, 579 (1973).
  - <sup>9</sup>W. J. Wiegand and W. L. Nighan, *Appl. Phys. Lett.* **22**, 583 (1973).
  - <sup>10</sup>Use of convectively cooled discharges reduces the importance of spatial variations in gas temperature and maintains the gas-mixture purity by minimizing the concentration of naturally occurring dissociation products, thereby facilitating comparison of experimental data with the theoretical predictions. The term *fast-flow* is used here to distinguish discharges cooled by convection from *slow-flow* or sealed discharges in which energy is removed by thermal conduction to the walls.
  - <sup>11</sup>W. L. Nighan, *Phys. Rev. A* **2**, 1989 (1970).
  - <sup>12</sup>J. J. Lowke, A. V. Phelps, and B. W. Irwin, *J. Appl. Phys.* **44**, 4664 (1973).
  - <sup>13</sup>The importance of multistep ionization as regards discharge instability is discussed in the Appendix. Strong electron-density-dependent ionization rates are not likely for the glow discharges investigated here, although two-step ionization involving the  $N_2(A^3\Sigma_u^+)$  and  $O_2(a^1\Delta_g)$  states and perhaps other metastables can be important in some circumstances. See Refs. 9 and 14.
  - <sup>14</sup>S. N. Foner and R. L. Hudson, *J. Chem. Phys.* **25**, 601 (1956).
  - <sup>15</sup>D. Rapp and P. Englander-Golden, *J. Chem. Phys.* **43**, 1464 (1965).
  - <sup>16</sup>C. E. Melton, *J. Chem. Phys.* **57**, 4218 (1972). The ions  $H^-$ ,  $O^-$ , and  $OH^-$  are all produced from  $H_2O$  by dissociative attachment of electrons, with the rate coefficient for  $H^-$  production (Fig. 2) dominating by approximately a factor of 10.
  - <sup>17</sup>R. E. Fox, *J. Chem. Phys.* **32**, 285 (1960).
  - <sup>18</sup>F. H. Mehr and M. A. Biondi, *Phys. Rev.* **181**, 264 (1969).
  - <sup>19</sup>C. S. Weller and M. A. Biondi, *Phys. Rev.* **172**, 198 (1968).
  - <sup>20</sup>C. S. Weller and M. A. Biondi, *Phys. Rev. Lett.* **19**, 59 (1967).
  - <sup>21</sup>J. N. Bardsley and M. A. Biondi, in *Advances in Atomic and Molecular Physics*, edited by D. R. Bates and I. Esterman (Academic, New York, 1970), Vol. 6.
  - <sup>22</sup>J. B. Hasted, *Physics of Atomic Collisions* (American Elsevier, New York, 1972), 2nd ed., Chap. 7.
  - <sup>23</sup>R. E. Olson, *J. Chem. Phys.* **56**, 2979 (1972).
  - <sup>24</sup>P. M. Eisner and M. N. Hirsh, *Phys. Rev. Lett.* **26**, 874 (1971).
  - <sup>25</sup>J. R. Peterson, W. H. Aberth, J. T. Moseley, and J. R. Sheridan, *Phys. Rev. A* **3**, 1651 (1971).
  - <sup>26</sup>J. T. Moseley, W. H. Aberth, and J. R. Peterson, *J. Geophys. Res.* **77**, 255 (1972).
  - <sup>27</sup>N. G. Adams, D. K. Bohme, D. B. Dunkin, F. C. Fehsenfeld, and E. E. Ferguson, *J. Chem. Phys.* **52**, 3133 (1970).
  - <sup>28</sup>J. L. Moruzzi and A. V. Phelps, *J. Chem. Phys.* **45**, 4617 (1966).
  - <sup>29</sup>J. L. Moruzzi, J. W. Ekin, Jr., and A. V. Phelps, *J. Chem. Phys.* **48**, 3070 (1968).
  - <sup>30</sup>F. C. Fehsenfeld, E. E. Ferguson, and A. L. Schmeltekopf, *J. Chem. Phys.* **45**, 1844 (1966).
  - <sup>31</sup>F. C. Fehsenfeld, D. L. Albritton, J. A. Burt, and H. I. Schiff, *Can. J. Chem.* **47**, 1793 (1969).
  - <sup>32</sup>J. L. Mauer and G. J. Schulz, *Phys. Rev. A* **7**, 593 (1973).
  - <sup>33</sup>D. A. Parkes, *Trans. Faraday Soc.* **67**, 711 (1971).
  - <sup>34</sup>D. A. Parkes, *Trans. Faraday Soc.* **68**, 627 (1972).
  - <sup>35</sup>R. Ranjan and C. C. Goodyear, *J. Phys. B* **6**, 1070 (1973).
  - <sup>36</sup>E. E. Ferguson, F. C. Fehsenfeld, and A. V. Phelps, *J. Chem. Phys.* **59**, 1565 (1973).
  - <sup>37</sup>J. A. Burt, *J. Chem. Phys.* **59**, 1567 (1973).
  - <sup>38</sup>L. J. Denes and J. J. Lowke, *Appl. Phys. Lett.* **23**, 130 (1973).
  - <sup>39</sup>W. J. Wiegand, M. C. Fowler, and J. A. Benda, *Appl. Phys. Lett.* **16**, 237 (1970).
  - <sup>40</sup>J. P. Reilly, *J. Appl. Phys.* **43**, 3411 (1972); C. A. Fenstermacher, M. J. Nutter, W. T. Leland, and K. Boyer, *Appl. Phys. Lett.* **20**, 56 (1972); J. S. Levine and A. Javan, *Appl. Phys. Lett.* **22**, 55 (1973).
  - <sup>41</sup>The clustering reaction leading to  $CO_3^-$  is intermediate between third and second order at the pressures considered here. The measured saturated three-body rate coefficient  $kM$  is several times  $10^{-10}$   $cm^3$   $sec^{-1}$  (Ref. 34).
  - <sup>42</sup>L. Pekarek, *Usp. Fiz. Nauk* **94**, 463 (1968) [*Sov. Phys.—Usp.* **11**, 188 (1968)], and references cited therein; L. Pekarek and V. L. Exner, *Rev. Roum. Phys.* **13**, 121 (1968).
  - <sup>43</sup>H. Sabadil, *Beitr. Plasma Phys.* **8**, 299 (1968).
  - <sup>44</sup>H. W. Rundle, K. A. Gillespie, R. M. Yealland, R. Sova, and J. M. Deckers, *Can. J. Chem.* **44**, 2995 (1966), and references cited therein.
  - <sup>45</sup>A. Garscadden, P. Bletzinger, and T. C. Simonen, *Phys. Fluids* **12**, 1833 (1969), and references cited therein.
  - <sup>46</sup>T. D. Rognlien and S. A. Self, *J. Plasma Phys.* **7**, 13 (1972).
  - <sup>47</sup>In the absence of electromagnetic phenomena such that  $\nabla \times \vec{E}_k = 0$ , application of Eq. (11) leads to the result  $\vec{E}_k \times \vec{k} = 0$ , indicating that the first-order perturbation in the electric field is in the direction of  $\vec{k}$ . Further, when space-charge relaxation is quasisteady,  $\nabla \cdot \vec{J}_{ek} = 0$  when ion current can be neglected. This implies that  $\vec{J}_{ek} \cdot \vec{k} = 0$ , or that the first-order perturbation in electron current density is in the direction perpendicular to  $\vec{k}$ . [See J. L. Kerrebrock, *AIAA J.* **2**, 1072

(1964) and also Ref. 7.]

<sup>48</sup>The requirement  $(v_g k / \nu_u) \ll 1$  also corresponds to the condition  $(\omega_r / \omega_i) \ll 1$  so that for plasma properties of present interest  $\omega \approx i\omega_i$ .

<sup>49</sup>A. G. Engelhardt, A. V. Phelps, and C. G. Risk, *Phys. Rev.* **135**, A1566 (1964); R. D. Hake, Jr. and A. V. Phelps, *Phys. Rev.* **158**, 70 (1967).

<sup>50</sup>The linear perturbation analysis employed here to determine the causes of instability for the conditions near onset cannot be used to predict plasma properties corresponding to the shaded regions of Figs. 10 and 11. The final quasisteady state achieved after a time long compared to that during which disturbances first begin to grow is affected by numerous complex processes which are unimportant near the instability boundary.

<sup>51</sup>D. H. Douglas-Hamilton and S. A. Mani, *Appl. Phys. Lett.* **23**, 508 (1973).

<sup>52</sup>The principal experimental findings discussed here in connection with the 3.8-cm-diam cylindrical discharge were subsequently confirmed using a 5-cm by 15-cm rectangular discharge channel for which the assumption of volume loss domination is more readily satisfied.

<sup>53</sup>For experimental convenience, the permanent gas CO is usually employed as the detacher. Hydrogen has also been utilized with generally similar results. However, the use of H<sub>2</sub> introduces an additional complication due to its role in altering the nature of the ions and/or clusters. Other naturally occurring detaching species such as O, NO, and O<sub>2</sub>( $a^1\Delta_g$ ) are not readily handled or introduce unfavorable additional cluster-ion reaction channels.

<sup>54</sup>The operating voltage of the discharge containing

running striations is typically 25% below that of the corresponding recombination-dominated stable plasma, reflecting an enhanced ionization rate in the unstable discharge. An explanation for this observation is that in the striated discharge a spatial and temporal average ionization rate sufficient to balance losses is provided by electrons accelerated in the high electric fields associated with the striation structure itself. Thus electrons in portions of the striations have electron temperature values which can even exceed those of point *a* in Fig. 4, whereas the *E/n* inferred from the average discharge voltage is below the minimum value required to sustain a stable discharge plasma; i.e., below point *b* in Fig. 4. This interpretation has recently been confirmed by computations of the temporal variations of *E/n* associated with unstable discharges in gas mixtures similar to those of the present study [W. F. Bailey, W. H. Long, D. R. Pond, and A. Garscadden (private communication)]. These investigators have also corroborated the present analytical and experimental findings relative to striation removal by the addition of detachment agents.

<sup>55</sup>J. L. Moruzzi, *Bull. Am. Phys. Soc.* **19**, 149 (1974). Excited N<sub>2</sub> (probably vibrationally excited) may play an important role in removing O<sup>-</sup> under gas discharge conditions.

<sup>56</sup>L. Pekarek and M. Sicha, *Czech. J. Phys. B* **10**, 749 (1960).

<sup>57</sup>K. W. Gentle, *Phys. Fluids* **9**, 2203 (1966).

<sup>58</sup>L. Pekarek, K. Masek, and K. Rohlena, *Czech. J. Phys. B* **20**, 879 (1970).

<sup>59</sup>T. Ruzicka and K. Rohlena, *Czech. J. Phys. B* **22**, 906 (1972).